

NACA TN 2888

# NATIONAL ADVISORY COMMITTEE FOR AERONAUTICS

TECHNICAL NOTE 2888

**CASE FILE  
COPY**

PERFORMANCE CHARACTERISTICS OF PLANE-WALL

TWO-DIMENSIONAL DIFFUSERS

By Elliott G. Reid

Stanford University

FEB 16 1953

PROPERTY FAIRCHILD  
ENGINEERING LIBRARY



Washington

February 1953

# TABLE OF CONTENTS

	Page
SUMMARY . . . . .	1
INTRODUCTION . . . . .	2
SYMBOLS . . . . .	7
APPARATUS AND TECHNIQUE . . . . .	9
TESTS . . . . .	14
DEFINITION AND INTERPRETATION OF PERFORMANCE PARAMETERS . . . . .	15
RESULTS AND ACCURACY . . . . .	22
DISCUSSION . . . . .	22
General Flow Characteristics . . . . .	24
Pressure-Recovery Characteristics . . . . .	29
Volumetric Efficiency and Effective Area Ratio . . . . .	36
Effects of Modifications . . . . .	38
CONCLUSIONS . . . . .	43
REFERENCES . . . . .	45
TABLES . . . . .	47-49
FIGURES . . . . .	50-80

NATIONAL ADVISORY COMMITTEE FOR AERONAUTICS

---

TECHNICAL NOTE 2888

---

PERFORMANCE CHARACTERISTICS OF PLANE-WALL

TWO-DIMENSIONAL DIFFUSERS

By Elliott G. Reid

SUMMARY

Experiments have been made at Stanford University to determine the performance characteristics of plane-wall, two-dimensional diffusers which were so proportioned as to insure reasonable approximation of two-dimensional flow.

All of the diffusers had identical entrance cross sections and discharged directly into a large plenum chamber; the test program included wide variations of divergence angle and length. During all tests a dynamic pressure of 60 pounds per square foot was maintained at the diffuser entrance and the boundary layer there was thin and fully turbulent.

The most interesting flow characteristics observed were the occasional appearance of steady, unseparated, asymmetric flow - which was correlated with the boundary-layer coalescence - and the rapid deterioration of flow steadiness - which occurred as soon as the divergence angle for maximum static pressure recovery was exceeded.

Pressure efficiency was found to be controlled almost exclusively by divergence angle, whereas static pressure recovery was markedly influenced by area ratio (or length) as well as divergence angle. Volumetric efficiency diminished as area ratio increased and at a greater rate with small lengths than with large ones. Large values of the static-pressure-recovery coefficient were attained only with long diffusers of large area ratio; under these conditions pressure efficiency was high and volumetric efficiency low.

Auxiliary tests with asymmetric diffusers demonstrated that longitudinal pressure gradient, rather than wall divergence angle, controlled flow separation. Others showed that the addition of even a short exit duct of uniform section augmented pressure recovery. Finally, it was found that the installation of a thin, central, longitudinal partition suppressed flow separation in short diffusers and thereby improved pressure recovery.

## INTRODUCTION

The experimental investigation reported herein was conceived as the first element of a broad research program directed toward the following objectives: To identify the conditions upon which diffuser performance is principally dependent, to determine their influences, and to utilize this information in the development of improved diffusers.

While the elevation of diffuser efficiency without regard for dimensional limitations is obviously desirable, the most welcome improvement from the aircraft designer's viewpoint would be the reduction of current lengths without sacrifice of efficiency. Special interest is therefore attached to diffusers with large rates of divergence.

Since diffusers have long been widely used, the necessity of seeking the first of the objectives stated above may seem somewhat anomalous. In most technical fields, the *modus operandi*, capacity, and limitations of commonly used devices are usually well-known before they have been so used for more than a decade. Unfortunately, this is not true of diffusers - although they have been used for more than a century.<sup>1</sup> As a matter of fact, although the lack of fundamental information on this subject has become increasingly apparent in recent years, relatively little new light has been shed upon diffuser performance during the 40 years which have elapsed since Professor A. H. Gibson completed his now-classic experiments (references 1 and 2). To bring this situation into sharp focus, a brief outline of the present state of knowledge regarding diffusers is presented herewith.

The availability of several competent digests of existing diffuser literature - notably the one by Patterson (reference 3) - makes it unnecessary to outline, here, much more than the boundaries of that information and, as implied above, this requires but few additions to a résumé of Gibson's work. In that résumé, however, emphasis is given to an aspect of the work which the writer believes to have received undeservedly scant attention in the past.

The diffuser investigation usually associated with Gibson's name consisted in the testing - with water - of three families of linearly tapered diffusers which had circular, square, and rectangular cross sections, respectively. (The rectangular ones were of two-dimensional form, i.e., they had two parallel, and two divergent, walls.) Area ratios  $R$  of 2.25, 4, and 9 were incorporated in the circular and rectangular types, whereas all the models of square section had area ratios of 4. In each case, models of various lengths provided coverage of the range of wall divergence angles  $2\theta$  between small values and  $180^\circ$ .

---

<sup>1</sup>Uriah Boyden (1804-1871) is generally credited with introduction of the diverging discharge tube as an adjunct to the water turbine.

Despite some shortcomings of technique - as seen from the modern viewpoint - the results of these tests indicated that the diffusers of all three types were characterized by sharply defined minimums of head loss which occurred at divergence angles  $2\theta$  between  $5.5^\circ$  and  $11^\circ$ , that the head losses increased rapidly toward the theoretical values corresponding to sudden enlargement of section as the divergence angles exceeded their optimum values, and that the losses in comparable diffusers were least for the circular, and the greatest for the rectangular, cross sections. These general characteristics have been repeatedly verified by others and no significant errors in Gibson's quantitative data have yet come to light.

Upon completion of this outstanding - but, nonetheless, essentially routine - exploratory study, Gibson embarked upon an investigation of more fundamental character. Unable to deduce, a priori, the optimum longitudinal distribution of cross-sectional area for a diffuser, he investigated the characteristics of the three curved-wall types which appeared to him most promising. The first was so designed that, if the flow were frictionless, the retardation  $dV/dt$  would be constant throughout the length of the diffuser; the resulting form is best described as "trumpet-shaped." The second, which had a less-pronounced flare, was characterized by constancy of the ideal value of  $dV/dx$ . The third was designed by an empirical method<sup>2</sup> intended to provide uniform loss of head per unit length; the wall curvature of this type was the least of the three.

Only three models of the first two types were tested because no significant improvement was effected. However, 13 models of the uniform-head-loss type - 6 of circular section and 7 rectangular, two-dimensional ones - were built and tested and all of them proved superior to the comparable linearly tapered diffusers. It is unfortunate that the effective divergence angles of these curved-wall diffusers were greater than those at which minimum head loss occurred in their linearly tapered counterparts because this precludes the direct comparison of relative merits under optimum conditions. However, the measured reductions of head loss ranged from 16 to more than 50 percent and conservative extrapolation of the corresponding experimentally determined curves leaves little doubt of the superiority of the uniform-head-loss type even under optimum conditions.<sup>3</sup>

---

<sup>2</sup>Based on the experimentally determined relationship between head loss and divergence angle for linearly tapered diffusers; for details, see pp. 106-108, reference 2.

<sup>3</sup>Ackeret (reference 4) tested two very similar curved-wall diffusers and obtained results consistent with those of Gibson.

The fundamental importance of this phase of Gibson's work is found in neither the development of an optimum diffuser form - for there is no evidence that this was accomplished - nor the considerable improvement of efficiency which was achieved, but rather in the demonstration that the efficiency of a diffuser of given length and area ratio is substantially influenced by variations in the longitudinal distribution of cross-sectional area. It also seems worth noting, specifically, that the foregoing results clearly show the linearly tapered type of diffuser to be endowed with no special virtue except simplicity of form.

At this point, attention is drawn to the striking analogy between the diffuser of fixed length and area ratio and the airfoil of specified camber and maximum thickness. Recognizing the fact that Gibson's study of diffuser profiles was a preliminary one which has never been systematically extended, it appears not unfair to appraise the present state of knowledge regarding diffusers as no better than that which prevailed in the case of airfoils just prior to the investigations which yielded the low-drag and high-critical-speed profiles now in common use. Thus the principal necessity of the first undertaking of the present program is found in the fact that, as of today, the effects upon performance of varying the longitudinal distribution of cross-sectional area in a diffuser of fixed over-all proportions are neither comprehensively known nor thoroughly understood.

While the foregoing comments do not imply that there has been little progress in diffuser research since Gibson's work was published, it does appear that attention has been largely diverted from the properties of simple diffusers and concentrated upon auxiliary devices intended to overcome their apparent deficiencies. Of these auxiliaries, boundary-layer control, entry guide vanes, and rotation vanes appear to deserve individual comments here.

Perhaps the most influential deterrent to further research on plain diffusers is the success with which suction boundary-layer control has been applied to the suppression of flow separation in short, wide-angle diffusers. The effectiveness of this arrangement, originally suggested by Prandtl in 1904 (reference 5), has been demonstrated by Schrenk (reference 6), Ackeret (reference 4), and more recently by Biebel (reference 7). While it has almost unlimited possibilities, the use of boundary-layer control involves the provision of auxiliary ducting and either a blower or some other suction-producing device of adequate capacity. These are complications which aircraft designers have, thus far, been unwilling to accept.

Some promising work with entry guide vanes has been done by Frey (reference 8), but its scope was so limited that the results are not generally useful. However, the attainment of pressure efficiencies of

52 and 47 percent with diffusers of  $R = 3$  and divergence angles  $2\theta$  of  $90^\circ$  and  $180^\circ$ , respectively, demonstrates that moderate pressure recovery can be had even in very short diffusers. While the effectiveness of such vanes in diffusers of moderate divergence is conjectural, investigation of this question appears well-warranted by Frey's results.

The idea of using fixed vanes to produce helical flow in a diffuser probably stemmed from earlier efforts to design efficient draft tubes for water turbines from which water is discharged with a vortexlike distribution of tangential velocity. Peters (reference 9) has shown that if a substantially uniform, that is, rigid body, rotation is superposed on the axial inflow of a conical diffuser, the pressure efficiency is considerably greater than that for simple translatory flow. A considerable part of this improvement may, of course, be ascribed to the fact that, since the spiral path is longer than the rectilinear one and the pressure rise per unit of path length correspondingly smaller, the introduction of the tangential velocity is equivalent to increasing the length and thus reducing the effective divergence angle of the diffuser. However, the demonstrated improvement of the efficiency of a diffuser characterized by the optimum divergence angle for translatory flow cannot be thus explained and Patterson has suggested that it may arise from the radial pressure gradient which is peculiar to the spiral flow.

The practical significance of this work has been at least ambiguously, if not erroneously, interpreted by Patterson who concludes, in reference 3, that, "In a conical diffuser having an angle of expansion in the range  $15 \text{ deg.} \leq 2\theta \leq 50 \text{ deg.}$  an efficiency of 80 per cent can be obtained by superposing a 'rigid body' rotation on the axial flow." Since the vanes used by Peters were installed well upstream from the diffuser entrance and the efficiencies computed from data obtained at the entrance and at a station in the exit duct, these efficiencies are based on the existence of helical flow at the entrance and take no account of the energy lost in the production of the tangential velocity. Thus Peters' experiments demonstrate only that, if appropriate spiral flow exists at the entrance of a conical diffuser, the efficiencies cited by Patterson may be obtained and they do not prove that the efficiency of a given diffuser may be augmented by installing within it rotation-producing vanes. This possibility is, however, one worth investigation and a basis for the expectation of some improvement is seen in the high efficiencies obtained by Peters with diffusers having large angles of divergence. An additional possibility which deserves consideration is that of recovering energy from the tangential motion by the use of counterrotation vanes at the diffuser exit.

Because of their bearing upon the character of the present experiments, two additional items must be included in this résumé; they concern the influences which the entrance boundary layer and the exit duct exert upon the efficiency of a diffuser.

The former can be described quite simply: It has been demonstrated - perhaps most thoroughly by Peters (reference 9) - that the pressure efficiency of a diffuser diminishes as the thickness of its entrance boundary layer increases. The effect is most pronounced when the layer is very thin and tends to disappear as the thickness becomes large. These findings have been verified at high subsonic speeds by the work of Copp and Klevatt at the Langley Aeronautical Laboratory of the National Advisory Committee for Aeronautics; however, the results of this work are not yet generally available.

The character and origin of exit-duct influence have long been known. Gibson, for example, reported in reference 1 that, when a diffuser discharged into a uniform duct having the same cross section as the exit, maximum static pressure occurred not at the exit section but at some distance downstream in the duct and this fact has been verified by numerous others. Reduction in the duct of the nonuniformity of velocity with which the fluid leaves the diffuser is the cause of this subsequent pressure increase. While it has been fairly common practice to base efficiency and head-loss calculations upon this maximum, rather than the exit, pressure, such results are characteristics of a diffuser-duct combination and it is difficult, if not impossible, to determine the characteristics of the isolated diffuser from those of the combination. This has been pointed out by Persh in connection with work done at the Langley Aeronautical Laboratory of the NACA, for which the results are not yet generally available, and further information on the matter will be found in the present report.

It will be apparent from the material which has been summarized above that the task of identifying the conditions upon which diffuser performance is principally dependent amounts to bridging the gap between Gibson's incomplete investigation of the influence of the longitudinal distribution of cross-section area upon performance and the more recent efforts to bypass this problem by incorporating auxiliary devices in conventional diffusers of simple geometric form. As matters now stand, the necessity of resorting to auxiliary devices is conjectural because the performance limits of simple diffusers are still unknown.

The first task is, then, to identify and study the influences of the parameters which fix these limits. Subsequent determination of their optimum combinations and the corresponding diffuser characteristics will be required to furnish a sound basis for the appraisal of such additional improvements of performance as may be obtainable by the incorporation of auxiliary devices.

The present investigation was undertaken as the first step toward these ends. The experiments consisted, primarily, in testing a family of symmetrical, plane-wall, two-dimensional diffusers. (A few auxiliary



tests for which the apparatus was particularly suitable were also included in the program.) To minimize or eliminate extraneous influences and sources of uncertainty which have characterized previous work in this field, the following precautionary measures were taken:

(a) A very thin, fully turbulent boundary layer was provided at the diffuser entrance

(b) The distance between the parallel walls of the diffusers was made eight times the minimum distance between the divergent ones

(c) The apparatus was so arranged that the diffusers discharged directly into a large plenum chamber

(d) All tests were made at the same value of entrance dynamic pressure

This work was carried out in the Guggenheim Aeronautic Laboratory of Stanford University; it was sponsored and financed by the NACA.

#### SYMBOLS

$A_1$	cross-sectional area of diffuser entrance, square inches (128 sq in. in all cases)
$A_2$	cross-sectional area of diffuser exit, square inches
$R$	area ratio ( $A_2/A_1$ )
$R_e$	effective area ratio ( $\eta_v R$ )
$r$	local area ratio ( $A/A_1$ , where $A$ is local cross-sectional area)
$L$	length of diffuser side plate, inches
$l$	distance of side-plate orifice from diffuser entrance, inches
$x$	axial distance from diffuser entrance, inches ( $L$ , $l$ , and $x$ are measured from downstream face of bellmouth end frame (5) in figure 1)
$y$	distance from diffuser wall, inches
$W_1$	width of diffuser entrance, inches (4 in. in all cases)

$W_2$	width of diffuser exit, inches
$P$	distance between parallel walls of diffuser, inches
$\theta$	divergence angle of side plate, degrees (total divergence angle equals $2\theta$ )
$\Omega$	included angle of wedge, degrees
$\rho$	air density, slugs per cubic foot
$\sigma$	relative density of air
$V$	velocity, feet per second
$\bar{V}$	mean velocity, feet per second
$Q$	volumetric flow rate, cubic feet per second
$p$	static pressure, pounds per square foot
$q$	dynamic pressure, pounds per square foot ( $\rho V^2/2$ )
$P_t$	total pressure, pounds per square foot ( $p + q$ )
$P_R$	static-pressure rise in diffuser, pounds per square foot ( $p_2 - p_1$ )
$\Delta p$	reduction of static pressure with reference to entrance total pressure, pounds per square foot ( $p_{t1} - p$ )
$C_{PR}$	pressure-recovery coefficient ( $(p_2 - p_1)/q_1$ )
$C_{\Delta p}$	pressure coefficient ( $\Delta p/q_1$ )
$\eta_p$	pressure efficiency ( $C_{PR}/\left(1 - \frac{1}{R^2}\right)$ )
$\eta_v$	volumetric efficiency ( $Q/Q_1$ )
$\delta$	boundary-layer thickness, inches
$\delta^*$	boundary-layer displacement thickness, inches

Position subscripts identify -

- o region upstream from diffuser
- 1 diffuser entrance
- 2 diffuser exit

Miscellaneous subscripts denote -

- i ideal
- e equivalent

### APPARATUS AND TECHNIQUE

This investigation was carried out by utilizing the Eiffel chamber of the Stanford wind tunnel as a plenum chamber into which the diffusers, installed therein, discharge air drawn from the quiescent outer region through an entry bellmouth which protruded through a gasket-sealed aperture in the chamber wall. During the tests, a dynamic pressure of 60 pounds per square foot was maintained at the entrance of each diffuser by so regulating the tunnel speed as to provide the necessary reduction of pressure within the chamber.

The diffusers themselves were of plane-wall, two-dimensional form and were so oriented as to produce horizontal flow from east to west. They were formed by the combination of four flat plates with an entry bellmouth which terminated in a short, uniform-section channel of 4-inch width and 32-inch height. The horizontal roof and floor plates were rigidly attached to the bellmouth while the rotatable side plates were connected to the bellmouth by flexible hinges of thin sheet steel which formed smooth entry fillets (approximately circular arcs) at all divergence angles. Variations of exit area (area ratio) were effected by rotating the side plates about their hinges and length was progressively reduced by cutting off the originally long plates.

Attention is drawn to the fact that, as all of the diffusers had entrance cross sections of identical dimensions, the use of a fixed entry passage and the maintenance of a predetermined dynamic pressure at its downstream end provided uniformity of entrance conditions throughout the entire series of experiments.

Turning now to details of the apparatus, figure 1 illustrates the arrangement of a typical diffuser of the greatest length tested ( $L/W_1 = 21.75$ ). The floor of the Eiffel chamber, or balance room, designated (1), served as a foundation for the installation. To it was bolted the massive table (2) which, in turn, provided a rigid anchorage for the two vertical I-beams (3). A pair of horizontal steel bars (4) were screwed to the steel end frame (5) of the laminated, wooden bellmouth (6) and clamped to the I-beams in order to support the entrance structure in proper position with reference to the table. It will be noted that, except for the fabric gasket (7), the bellmouth was in no way connected to the chamber wall (8) which deflects appreciably under operating air loads. The sheet-metal fairings, or filler plates, (9) and the stiffened plywood faceplate (10) completed the fixed boundaries of the entrance channel.

A conveniently removable, semicylindrical screen (11), supported by a frame of wood and steel tubing, was fitted over the bellmouth and faceplate to insure uniform velocity and low turbulence of the entrant air stream. The screen was made of 0.0104-inch-diameter brass wire, woven 40 by 40 per inch. Figures 2 and 3 are photographs of the bellmouth and screen. In the former, the screen has been detached and elevated to give access to the diffuser entrance; in the latter, the screen is shown in the operating position. The contraction of the air stream between screen and diffuser entrance is also noteworthy. The screen area (height, 4 ft, diam., 5 ft) was 31.4 square feet, the diffuser entrance area (4 by 32 in.) was 0.89 square foot, and their ratio was 35.3:1.

The diffusers themselves consisted of a floor plate (12) - supported by the transverse frames (13) - two side plates (14), and the roof plate (15), pressed together by the compression bolts (16). The roof and floor plates were fastened to the bellmouth end frame by machine screws while the side plates were attached to it by means of the flexible hinges (17). Details of these hinges are shown in figures 1(b) and 4; the latter is a close-up photograph taken with one of the side plates removed. The hinge material was 2.5- by 0.015-inch blued-steel clock-spring stock; this was oven-sweated to the detachable element of the bellmouth end frame and to the steel edge member of the side plate. The free length of the hinge was 1.125 inches. Figure 5 is a rear-view photograph of a diffuser of the same length as, but of greater area ratio than, the one detailed in figure 1.

The diffuser plates were, actually, shallow box beams built up by gluing and screwing heavy plywood plates to cellular wooden frames, each of which consisted of four longitudinal and seven transverse members. The air-flow surfaces of these plates, as well as those of the bellmouth and its faceplate, were filled, sanded, lacquered, and rubbed to a high

polish. Great care was taken to obtain smooth joints between bellmouth, end frame, hinges, and plates; exploration with a feeler gage indicated that surface discontinuities at these joints did not exceed 0.0015 inch. To prevent air leakage, the upper and lower edges of the side plates were faced with felt and the top and bottom edges of the hinges were sealed externally with Plasticine.

Accurate positioning of the side plates was complicated by the flexibility of the hinges and weight of the plates. Early trials proved that equal displacements of the downstream ends of the side plates from the vertical plane of symmetry did not insure symmetry of the diffuser entrance - for the upstream ends of the plates would not always move equally. To preclude such asymmetry during the tests, the forward ends of the side plates were individually positioned by use of a dial gage in a fixture which utilized the plane walls of the downstream section of the bellmouth as reference surfaces. The gage settings were obtained from curves of side-plate displacement (in a transverse plane just beyond the hinge) against exit width; the coordinates of the curves for the various diffuser lengths were determined by calculations based on the assumption of circular-arc hinge form. A gage tolerance of  $\pm 0.003$  inch, as measured after clamping the plates, was observed throughout the test program.

To obtain the desired test data, means were provided for determination of the total pressure of the entering air stream, the static pressure at the diffuser entrance, the distribution of pressure along the center lines of the divergent side plates, and the distribution of total pressure over the exit cross section. All of these pressures were measured with reference to the static pressure in a region of the plenum chamber which was undisturbed by the diffuser discharge.

As the total pressure of the air just inside the screen differed from the static pressure there by less than  $0.001q_1$  (because the contraction ratio was 35.3), measurement of the latter served to determine the former with negligible error. For this purpose, three flush orifices were located near the outer edge of the upper plate of the entrance screen structure and interconnected by the tubes which may be seen in figure 3.

Twelve static orifices were distributed, symmetrically, around the perimeter of a bellmouth cross section located  $1/2$  inch upstream from the steel end frame. They served three purposes: To determine the velocity distribution at the diffuser entrance,<sup>4</sup> to guide and support the hypodermic tube used for boundary-layer surveys, and to enable

---

<sup>4</sup> Actually 1.25 in. upstream from the foremost point of hinge flexure.

regulation of the entrance dynamic pressure during tests. One of these orifice installations is shown in figure 1(b).

Twenty-five orifices were identically distributed along the horizontal center line of each of the rotatable side plates; their locations are given in table I and a typical installation is detailed in figure 1(b). Each pair of rubber tubes from corresponding orifices in the two plates was led through a three-roller, multiple pinch clamp and thence, through a Y-connector, to a single tube of the recording manometer. A half turn in either direction of the eccentrically mounted central roller of the pinch clamp caused simultaneous closure of all of the tubes leading to one or the other side plate and thus enabled convenient inspection, comparison, and recording of the distributions of pressure along the center lines of the two plates.

Surveys of total pressure at the discharge ends of the diffusers were made by use of a horizontal, rotatable rake attached to a carriage which could be traversed vertically along a rail fastened to the downstream end of the north side plate.<sup>5</sup> This movable assembly is shown in figure 6; the rake, itself, consists of a brass bar of NACA 0025 profile and 1.75-inch chord, from the leading edge of which project 16 total-pressure tubes of 0.058-inch diameter and 1.625-inch length. During the tests, care was taken to locate the tips of the tubes within 0.03 inch of the exit plane. As relatively large diffuser divergence angles were anticipated, the tips of the total-pressure tubes were cupped to minimize errors due to flow inclination; the yaw characteristics of similarly shaped tubes are compared with those of conventional ones in figure 7.

It will be noted that the spacing of tubes along the rake is non-uniform. This unfortunate arrangement was adopted with the object of obtaining the best possible definition of the boundary layer of one plate - and with the naive expectation that the flow would be substantially symmetrical in diffusers of all useful proportions. The unexpected occurrence of markedly asymmetric flow under some conditions of relatively high pressure efficiency therefore resulted in rather incomplete definition of the distribution of total pressure over the south half of the exit cross section in these cases.

Preliminary testing consisted in exploration and adjustment of the velocity distribution and boundary-layer characteristics at the downstream end of the bellmouth.

Work was begun with the original bellmouth in which the profiles of the horizontal and vertical segments were identical. Measurement of the static pressures at the 12 orifices previously described indicated

---

<sup>5</sup>The north plate appears on the left in photographs taken from the discharge end.

excessive vertical contraction of the stream, that is, the velocity was minimum at midheight and maximums were found near the top and bottom of the cross section. Temporary fairings, or filler plates, were therefore installed to reduce vertical contraction within the bellmouth. These fairings were empirically modified until satisfactory uniformity of the static pressure was obtained at the downstream end of the bellmouth, and permanent metal plates of the final form were then installed. The velocity distribution thus obtained is illustrated by figure 8.

With the bellmouth in its finally fixed form, preliminary surveys of the entrance boundary layer were made. The instrument used for this purpose is shown in figure 9. It consists, essentially, of a short length of hypodermic tubing with a specially formed tip which projected into the air stream through one of the static orifices at the downstream end of the bellmouth and a micrometer positioning device which fitted over the orifice connection and was screwed to the outer surface of the bellmouth. A rubber-disk compression coupling in the spring-restrained, movable element of the positioning device enabled transmission of the total pressure at the tip of the exploring tube to the recording manometer. The tip of the hypodermic tube was so flattened and ground that the center of the aperture, which measured 0.011 by 0.0045 inch, could be brought within 0.006 inch of the bellmouth wall.

The first surveys made indicated that, although the boundary layer was unmistakably turbulent at some stations, transition was still incomplete at others. (This conclusion was drawn from the forms of the curves of velocity against distance from the wall when plotted in logarithmic coordinates.) The substantial uniformity of the thin, fully turbulent boundary layer defined by the velocity profiles of figure 10 was obtained by lacquering a fine silk thread (0.008-in. diam.) to each of the vertical surfaces of the bellmouth at a distance of 4 inches upstream from the plane of exploration.

The entrance velocity distribution and boundary-layer profiles of figures 8 and 10 were determined under the condition  $q_1 = 60$  pounds per square foot; this value corresponds to an entrance velocity of approximately 155 miles per hour for air of the average density found in the laboratory, that is,  $\sigma \approx 0.95$ . Since this dynamic pressure was maintained during the subsequent recording of all test data, figures 8 and 10 depict the conditions which prevailed just upstream of the entrances of all of the diffusers tested during this investigation.

A double bell-jar balance of high sensitivity ( $\pm 0.02$  lb/sq ft) was used to measure the entrance dynamic pressure  $q_1$ . Relatively rapid response of this balance was obtained by connecting one of the bell jars, through a multiple connector, to six of the static orifices at the diffuser entrance  $p_1$  and by similarly connecting the other one to the

three orifices just inside the inlet screen  $p_{to}$ . The pressures in the two bell jars were transmitted, through T-connections, to the recording manometer.

Despite these precautions, the manometer column connected to the orifices at the diffuser entrance failed to follow the static-pressure fluctuations which occurred in diffusers of excessive divergence angle. To preclude the recording of data during excursions of  $p_1$  from the average value indicated by the balance and its connected manometer column, an adjacent column was connected directly to one of the orifices at the diffuser entrance and records were taken only when the heights of these two columns were in close agreement.

All pressures were photographically recorded and were reduced directly to nondimensional pressure ratios by use of a special optical scaling device.

### TESTS

The primary objective of the present experimental program was to determine the performance characteristics of symmetrical, plane-wall, two-dimensional diffusers throughout the practically useful ranges of the length ratio  $L/W_1$  and the area ratio  $R$ . Secondary objectives were to explore the influence of asymmetry and to determine the effects of adding constant-section extensions and internal partitions to diffusers of the symmetrical type.

The major element of the program consisted in testing 22 symmetrical models of the proportions tabulated below:

$L/W_1$	$R$
21.75	2, 3, 4, 5
15.25	2, 3, 4, 5
11.00	2, 2.5, 3, 3.5, 4
7.75	1.8, 2, 2.5, 3, 3.5
5.50	1.75, 2, 2.25, 2.625

These will be referred to, hereafter, as the "plain diffusers," to distinguish them from the other types described below.



The effect of asymmetry was investigated by alining one (the south) side plate with the direction of the entrant stream and varying the divergence angle of the other plate to obtain the desired area ratio. These tests were made with  $L/W_1 = 7.75$  and at area ratios  $R$  of 2, 2.5, and 3.

Constant-section (parallel side-wall) extensions were added to plain diffusers of  $L/W_1 = 11$  and  $R = 2$  and 3.5 by reattaching the side-plate segments which had been cut off to reduce  $L/W_1$  from 15.25 to 11.00. The roof and floor plates remained uncut at  $L/W_1 = 15.25$  during these tests.

The first type of divided diffuser to be investigated was formed by installing a central partition of 1/8-inch aluminum plate in a plain diffuser of  $L/W_1 = 7.75$ . This plate, which may be seen in figure 11, extended 2 inches upstream from the foremost point of hinge flexure and had a semicircular leading-edge profile. Instability of the relatively flexible plate necessitated use of the lateral supports visible in figure 11; these consisted of 1/8- by 3/4-inch rectangular aluminum-alloy bars which were notched to slip over the edges of the plate. The two at the leading edge had no end fittings and were simply wedged between the parallel walls of the bellmouth while the downstream ones were screwed to external blocks as may be seen in the photograph. Tests were made of this arrangement with  $R = 2.5, 3$ , and 3.5.

The second type of divided diffuser differed from the first by the substitution of a wedge for the thin plate. The wedge consisted of a Masonite covered wooden frame with a solid-maple leading-edge strip. The vertex of the wedge was truncated and rounded to a 1/8-inch radius; the foremost point of the rounded nose was located 2.2 inches downstream from the diffuser entrance (foremost point of hinge flexure) and the wedge terminated at the diffuser exit. Tests were made with the side plates swung out far enough to provide unobstructed exit areas of 2.5 and 3 times the entrance area ( $R = 2.5$  and 3) with  $L/W_1 = 7.75$ .

#### DEFINITION AND INTERPRETATION OF PERFORMANCE PARAMETERS

Physical interpretation of the parameters used in presentation of the experimental results will be facilitated by reference to figure 12.

The central diagram (fig. 12(b)) illustrates the variations of static, dynamic, and total pressures in a longitudinal section of a two-dimensional diffuser into which previously undisturbed air is drawn by reduction of pressure in the discharge plenum chamber - as in the present

tests. The static pressure at the exit  $p_2$  is necessarily equal to that in the plenum chamber. The flow-producing pressure difference is, therefore,  $\Delta p_2 = p_{t1} - p_2$  and, if entrance losses are negligible,  $\Delta p_2 = p_{t0} - p_2$ . The kinetic energy of the discharged stream is, of course, dissipated by turbulent mixing with the air in the plenum chamber. The static pressure recovered within the diffuser is  $p_R = p_2 - p_1$ .

In the case of such a streamline as A, the total pressure remains unchanged (at the value  $p_{t0}$ ) throughout the length of the diffuser and does not diminish until the streamline enters the external mixing zone. On the other hand, a loss of total pressure within the diffuser characterizes all streamlines such as B which traverse any part of the wall boundary layers. The velocity of efflux in the case of streamline A is identical with that for a frictionless fluid of the same density as the air, that is,

$$V_{2A} = \sqrt{2q_{2A}/\rho} = \sqrt{2\Delta p_2/\rho} = V_{2i} \quad (1)$$

whereas the smaller discharge velocity

$$V_{2B} = \sqrt{2q_{2B}/\rho} < \sqrt{2\Delta p_2/\rho} = V_{2i} \quad (2)$$

prevails in the case of streamline B. The exit velocity profile is shown at the downstream end of the diffuser in diagram 12(b); at the exit the displacement thickness of the boundary layer is  $\delta^*_2$  and the volumetric flow rate (per unit distance normal to the plane of flow) is

$$Q = V_{2i}(W_2 - 2\delta^*_2) \quad (3)$$

If one now imagines  $p_2$  (and  $\Delta p_2$ ) to remain unchanged while the viscosity of the air and, therefore, the boundary-layer thickness diminish indefinitely, maintenance of the previously established value of  $Q$  would necessitate reduction of the exit width by the amount of the reduction of total boundary-layer displacement thickness at the exit. Thus, as the viscosity approached zero, the exit width would approach the limiting value  $W_2 - 2\delta^*_2$ . Furthermore, reduction of the diffuser width throughout its length by amounts equal to the local displacement thicknesses would leave both the longitudinal distribution of static pressure and the volumetric flow rate unchanged by the elimination of viscosity.

Thus the volumetric flow rate and longitudinal distribution of static pressure in a real diffuser are those which would characterize frictionless flow through a diffuser whose transverse dimensions were smaller than those of the real one by the local thickness of the wall boundary layers. Such an idealized "equivalent" diffuser is shown in diagram 12(c).

If the foregoing reduction of viscosity were not accompanied by any change of the dimensions of the diffuser, the uniformity of exit velocity - at the value  $V_{2i}$  - would result in an increase of the volumetric flow rate and in a corresponding reduction of the static pressures at all points upstream from the exit. The consequences of such ideal flow through the real diffuser are illustrated by diagram 12(a).

These concepts suggest expression of the experimentally determined static-pressure rise within a diffuser in the form of a nondimensional coefficient and the comparison of its value with that of the corresponding ideal one. The pressure-recovery coefficient is defined as

$$C_{PR} = \frac{p_2 - p_1}{q_1} \quad (4)$$

The experimental results serve to define  $C_{PR}$  as a function of the area ratio  $A_2/A_1 = R$  and the length ratio  $L/W_1$ .

To derive the formula for the ideal pressure-recovery coefficient, rewrite the perfect-fluid form of Bernoulli's equation

$$p_1 + q_1 = p_2 + q_2 \quad (5)$$

$$\frac{p_2 - p_1}{q_1} = 1 - \frac{q_2}{q_1} \quad (6)$$

and substitute for  $q_2/q_1$  in accordance with

$$\frac{q_2}{q_1} = \left( \frac{V_2}{V_1} \right)^2 = \left( \frac{A_1}{A_2} \right)^2 = \frac{1}{R^2} \quad (7)$$

Thus, in the ideal flow

$$\frac{p_2 - p_1}{q_1} = 1 - \frac{1}{R^2} \quad (8)$$

and, since

$$C_{PRi} = \left( \frac{p_2 - p_1}{q_1} \right)_i \quad (9)$$

the result is

$$C_{PRi} = 1 - \frac{1}{R^2} \quad (10)$$

The ideal value is thus seen to be independent of the length of the diffuser and to depend only upon the area ratio.

Since comparisons are to be made between the present results and those of previous experiments, the relation between pressure efficiency - in terms of which most of the latter are presented - and the coefficient  $C_{PR}$  is derived below. Pressure efficiency is defined as

$$\eta_p = \frac{p_2 - p_1}{\frac{\rho V_1^2}{2} \left[ 1 - \left( \frac{A_1}{A_2} \right)^2 \right]} \quad (11)$$

The introduction of  $q_1 = \rho V_1^2 / 2$  and  $R = A_2 / A_1$  yields the alternative forms

$$\eta_p = \frac{p_2 - p_1}{q_1 \left( 1 - \frac{1}{R^2} \right)} = \frac{(p_2 - p_1) / q_1}{\left( 1 - \frac{1}{R^2} \right)} \quad (12)$$

from the latter of which it is evident that

$$\eta_p = \frac{C_{PR}}{C_{PRi}} \quad (13)$$

Thus, pressure efficiency is merely the ratio of the actual pressure recovery to the ideal one.

Since the value of  $\eta_p$  is sometimes erroneously interpreted as an index of pressure recovery, it appears worth while to point out that this interpretation is valid only under special circumstances. This will be evident when the value of  $C_{PRi}$  from equation (10) is substituted in equation (13)

$$\eta_p = \frac{C_{PR}}{1 - \frac{1}{R^2}} \quad (14)$$

and the equation is rearranged in the form

$$C_{PR} = \eta_p \left( 1 - \frac{1}{R^2} \right) \quad (15)$$

It will be seen from equation (15) that the dependence of  $C_{PR}$  upon the value of  $R$ , as well as that of  $\eta_p$ , makes  $\eta_p$  useless as an index of pressure recovery unless the diffusers under consideration have equal area ratios. It is also evident that as  $R$  increases,  $C_{PR}$  will also increase so long as  $\eta_p$  does not diminish as rapidly as  $1 - (1/R^2)$  increases. For this reason - as will be demonstrated by the experimental results - the maximum value of  $C_{PR}$  for diffusers of a given length occurs at a value of  $R$  considerably larger than that at which  $\eta_p$  is maximum. These considerations are chiefly responsible for the introduction and use in this report of the pressure-recovery coefficients defined above.<sup>6</sup>

Another parameter useful in appraising the merits of various diffusers is the area ratio of the equivalent diffuser of figure 12(c). Since a real diffuser and its idealized equivalent are characterized by the same value of  $C_{PR}$ , the result obtained in equation (10) may be utilized to write

$$C_{PR} = C_{PRie} = 1 - \frac{1}{R_e^2} \quad (16)$$

---

<sup>6</sup>Peters (reference 9, p. 16) has pointed out the unsuitability of  $\eta_p$  as an indicator of the merits of diffusers of different area ratios. Both he and Gibson compare the actual loss to the theoretical loss due to sudden increase of cross-sectional area. However, as this limit has little significance unless large separation losses occur, coefficients of the present type appear preferable.

in which  $R_e$  is the area ratio of the equivalent diffuser. From equation (16) it is evident that

$$R_e = \sqrt{\frac{1}{1 - C_{PR}}} \quad (17)$$

An aspect of diffuser performance which appears to have received little or no attention in the past is the disparity between actual and ideal volumetric flow rates. This matter is of interest because the disparity may be of considerable magnitude even though the pressure efficiency is high or the pressure-recovery coefficient large. The relationships which underlie this anomalous state of affairs are developed, below, in terms of "volumetric efficiency" which is defined as

$$\eta_v = Q/Q_i \quad (18)$$

Since the volumetric rates of the viscous flow through a real diffuser and the frictionless flow through its idealized equivalent are identical under fixed conditions of operation,

$$Q = V_{2i} W_{2e} \quad (19)$$

because the exit velocity has the uniform value  $V_{2i}$  in the latter case. Similarly,

$$Q_i = V_{2i} W_2 \quad (20)$$

whence

$$\eta_v = \frac{W_{2e}}{W_2} = \frac{R_e}{R} \quad (21)$$

If the value of  $R_e$  given by equation (17) is now substituted in equation (21), it is found that

$$\eta_v = \frac{1}{R\sqrt{1 - C_{PR}}} \quad (22)$$

An alternative form of the relationship is obtained by substituting  $\eta_p \left(1 - \frac{1}{R^2}\right)$  for  $C_{PR}$  in accordance with equation (15); the result is

$$\eta_v = \frac{1}{\sqrt{R^2 - \eta_p(R^2 - 1)}} \quad (23)$$

Equations (22) and (23) indicate, as might be expected, that if  $R = \text{Constant}$ ,  $\eta_v$  will be augmented if either  $C_{PR}$  or  $\eta_p$  is increased. However, it is also evident that if either  $\eta_p$  or  $C_{PR}$  remains constant while  $R$  increases,  $\eta_v$  will be reduced. These relationships were deduced in the course of investigating apparently paradoxical experimental results which indicated that an increase in the divergence angle (area ratio) of a diffuser of fixed length caused an increase of  $\eta_p$  but a reduction of  $\eta_v$ . Examination of equation (23) reveals, of course, that this is bound to occur if the rate of increase of  $\eta_p$  is insufficient to compensate for that of  $R$ .

The foregoing definitions of, and relationships between, the various parameters are summarized below for convenience of reference:

$$R = A_2/A_1 \quad \text{In two-dimensional case } R = W_2/W_1$$

$$C_{PR} = \frac{P_2 - P_1}{q_1}$$

$$C_{PRi} = 1 - \frac{1}{R^2}$$

$$\eta_p = \frac{P_2 - P_1}{q_1 \left(1 - \frac{1}{R^2}\right)} = \frac{C_{PR}}{C_{PRi}}$$

$$R_e = \sqrt{\frac{1}{1 - C_{PR}}}$$

$$\eta_v = \frac{Q}{Q_i} = \frac{R_e}{R} = \frac{1}{R \sqrt{1 - C_{PR}}} = \frac{1}{\sqrt{R^2 - \eta_p(R^2 - 1)}}$$

## RESULTS AND ACCURACY

The experimental results for the 22 plain diffusers are tabulated, together with the geometric characteristics of these models, in table II. Similar data for the asymmetric, extended, and divided diffusers will be found in table III.

Auxiliary data presented only in graphical forms illustrate longitudinal distributions of static pressure, typical dynamic-pressure distribution at exit, and so forth. Specific reference to these charts and to various graphical presentations of the basic data will be found in the following section.

The accuracy of the test results is not uniform because the steadiness of flow through diffusers of all lengths deteriorated rapidly with increase of the divergence angles beyond the values at which maximum pressure recoveries were attained.

With diffusers of less-than-optimum divergence, it is believed that errors in pressure recording did not exceed  $\pm 0.01q_1$  for no greater discrepancy between the results of visual observations and photographic recording was found in these cases.

With reference to diffusers having greater-than-optimum divergence, it can be said only that every effort was made to record what appeared to be the mean characteristics of the fluctuating flows. Several (usually nine) photographic records were made of the entrance, wall, and exit static pressures in each diffuser because one record had to be made for each position of the exit survey rake. The first two records of each series were always completely scaled and, in the event of appreciable discrepancy between the resulting values of  $C_{PR}$ , the data from these and additional records were averaged to obtain a representative result. While the portions of the  $C_{PR}$  curves which these data define appear reasonably consistent, it is suspected that some of the pressures recorded for unsteady flows may differ from the true mean values by as much as  $0.03q_1$ .

## DISCUSSION

In order that the results of the present experiments may be properly interpreted and appraised, cognizance must be taken of some important differences between this investigation and previous studies of two-dimensional diffusers. The most significant ones are revealed by the



following tabulation in which previous work on the subject is listed chronologically.<sup>7</sup>

# SUMMARY OF TWO-DIMENSIONAL DIFFUSER RESEARCH

Research	$L/W_1$	$2\theta$ (deg)	R	$P/W_1$ (1)	$P/W_2$ (1)
Gibson (1910, 1911 - references 1 and 2)	2.4-7.2 4.4-34.4 5.7-45.9	10-30 5-40 10-90	2.25 4.00 9.00	1.0 1.0 2.25	0.44 .25 .25
Vedernikoff (1926 - reference 15)	1.0	0-26	1.0-7.77	1.0	1.0-0.13
Nikuradse (1929 - reference 10)	33.3	0-8	1.0-5.65	25.0	25.0-4.42
Demontis (1936 - reference 16)	3.5	0-31	1.0-2.94	1.0	1.0-0.34
Polzin (1940 - reference 17)	15.0	0-44	1.0-11.9	1.0	1.0-0.084
Present investigation (1950)	5.50 7.75 11.00 15.25 21.75	8.0-17.4 6.0-18.9 5.4-15.9 3.8-15.2 2.7-10.7	1.75-2.625 1.8-3.5 2.0-4.0 2.0-5.0 2.0-5.0	8.0 8.0 8.0 8.0 8.0	4.57-3.04 4.45-2.63 4.0-2.0 4.0-1.6 4.0-1.6

<sup>1</sup><sub>P</sub>, distance between parallel walls.

The first point clarified by these data is that no one but Gibson has investigated the effect of length ratio  $L/W_1$  upon the performance of diffusers of either fixed area ratio or fixed divergence angle. In each of Gibson's three families of diffusers, the area ratio remained constant and variations of divergence angle were obtained by building

<sup>7</sup>All significant previous studies of two-dimensional diffusers are believed to be included in this list. Göttingen work prior to that of Nikuradse is omitted in view of his summary and criticism (in reference 10) of the experiments carried out by Andres (reference 11), Hochschild (reference 12), Kröner (reference 13), and Dönch (reference 14).

models of different lengths. The fact that each of the later experimenters varied only the divergence angle of a diffuser of fixed length is not readily explainable for, although Gibson concluded - in effect - that pressure efficiency depended principally upon divergence angle, his result showed that variations of length had considerable effects when the divergence angle was fixed.

The second, and perhaps even more surprising, feature of this summary is the revelation that, in all previous work except that of Nikuradse, the proportions of the diffuser cross sections have been such as to preclude even close approximation of two-dimensional flow. This is apparent in the tabulated values of  $P/W_1$  and  $P/W_2$ ; it will be seen that most of the entrance cross sections were square and that, at the exit, the distance between the parallel walls exceeded that between the divergent ones only in the case of Nikuradse's experiments. Even more unfortunate are the facts that Nikuradse not only worked with a variable-angle diffuser of fixed length but was so exclusively concerned with boundary-layer phenomena that he neglected even to record the pressure recoveries obtained with that model.

Reference to the foregoing tabulation will now show that the present investigation is characterized by neither of the shortcomings mentioned above. It includes determination of the effects of both the area and length ratios and the proportions of the models are such that substantial deviations from two-dimensional flow are unlikely to occur in the absence of extremely thick boundary layers which, after all, connote large energy losses. It thus appears that the present investigation is the first comprehensive study of two-dimensional diffusers in which even approximately two-dimensional flow has prevailed.

The following discussion of the results of these experiments is divided into four sections which deal, respectively, with the general character of the flow through the diffusers, their pressure-recovery characteristics, the question of volumetric efficiency, and the effects of miscellaneous modifications.

### General Flow Characteristics

Since uniform velocity prevailed everywhere except within the thin boundary layer at the entrances of all the diffusers, the extent to which two-dimensional flow was subsequently maintained in any particular one can be readily appraised by inspection of the contours of equal dynamic pressure at its exit. Such contour charts for the longest and shortest of the diffusers tested are reproduced in the upper half of figure 13.

There it will be seen that the contours for diffusers of both lengths closely approach parallelism with the vertical boundaries of the exit cross sections throughout considerable portions of the diffuser height when the area ratios are small - for example, when  $L/W_1 = 5.50$ ,  $R = 1.75$  to  $2.25$  and when  $L/W_1 = 21.75$ ,  $R = 2.0$  to  $3.0$ . Flows which are substantially two-dimensional, therefore, prevail within these regions. Inspection alone may create the erroneous impression that serious deviation from two-dimensional flow is indicated by such contours as those for  $L/W_1 = 21.75$ ,  $R = 4.0$ . However, a few calculations will show that the variation of maximum discharge velocity among the horizontal sections which occupy the central half of the height of this diffuser is less than 10 percent. It is also worth noting that the curve of maximum velocity, while asymmetrically located, is relatively straight and nearly vertical throughout most of its length. The fact that the contour charts for the largest area ratio in each group, that is,  $L/W_1 = 5.50$ ,  $R = 2.625$  and  $L/W_1 = 21.75$ ,  $R = 5.0$ , even resemble those for diffusers of the same lengths and smaller area ratios is somewhat remarkable - for in both of these cases the flows were very unsteady and the contours represent transient conditions. (Some idea of the magnitude of the fluctuations may be obtained from the two successively recorded dynamic-pressure profiles which are reproduced below the contour chart for the shorter diffuser.)

Since the examples in figure 13 represent the extremes of the length and area ratios included in this investigation, and as the contour charts for models of intermediate proportions are consistent with those reproduced in figure 13, it is apparent that good approximation of two-dimensional flow was obtained with all of the diffusers in which steady flow prevailed and that this characteristic was retained to a considerable extent even when the divergence angle became so large that intermittent separation caused the flow to become unsteady.

While it is well-known that the general effects of continuously increasing the area ratio of a diffuser of given length are to produce, at first, mere thickening of the wall boundary layers, then intermittent separation - accompanied by fluctuations of flow pattern and entrance velocity - and, finally, complete separation and chaotic turbulence, the present experiments have shed further light on several aspects of these phenomena. One of these is the anomaly of continuous asymmetric flow in a symmetrical, two-dimensional diffuser.

Flows of this kind were encountered during the first preliminary tests which were necessarily made with very long diffusers ( $L/W_1 = 21.75$ ). This caused much concern and considerable delay because it was feared that some serious imperfection of the experimental apparatus had escaped detection or that an unsuitable orientation of the diffuser with reference

to the Eiffel chamber and tunnel air stream had been chosen. However, careful reexamination of the apparatus and the entrance velocity and boundary-layer survey data revealed no evidence of significant imperfection and auxiliary tests demonstrated that the asymmetry of flow was not substantially altered by such radical modifications of the test conditions as placing large obstructions near the inlet screen or installing an inclined plate close to the diffuser exit to deflect the discharge stream first toward one side and then the other.

At this juncture, a search of the literature was instituted with the object of discovering whether similar behavior of a two-dimensional diffuser had been reported by any previous experimenter. It was found that both Nikuradse and Demontis had observed the same puzzling phenomenon; the former dismissed it with little attention but the latter reported that somewhat extensive tests failed to reveal the cause. It was therefore assumed that the asymmetry was the result of some form of instability which stemmed from imperfections too slight to be readily detected and it was decided to proceed with the experiments without making further - and probably futile - efforts to eradicate the unknown source of the disturbance. The consistent displacement of the maximum velocity line which characterized all of the diffusers with  $L/W_1 = 21.75$  is evident in the corresponding contours and dynamic-pressure profiles of figure 13.

As the diffuser length was progressively reduced during subsequent tests, it was noticed that asymmetry of the exit flow at midheight became less pronounced and later disappeared when small area ratios were used - even though marked asymmetry persisted near the parallel walls. Moreover, it appeared that the exit velocity distribution was symmetrical in all horizontal sections in which the dynamic-pressure ratio  $q_2/q_{2i}$  attained a value of unity. Now, since  $q_2 = q_{2i} = \Delta p$  on all streamlines which do not traverse any part of the boundary layer (see fig. 12), this observation suggested that asymmetry must be confined to those sections which lie entirely within the boundary layer.

Examination of the exit survey data for all of the diffusers has confirmed the validity of this hypothesis in all cases of steady flow. Typical results which illustrate the conspicuous symmetry of the discharge from short diffusers which are characterized by relatively thin boundary layers and a central core of undiminished total pressure are the diagrams of figure 13 which correspond to  $L/W_1 = 5.50$  and  $R = 1.75$  to  $2.25$ . It will be noted that their midheight dynamic-pressure profiles have maximum ordinates of 1.0, a characteristic not exhibited by any of the profiles for the diffusers with  $L/W_1 = 21.75$ . It thus appears that in a symmetrical, two-dimensional diffuser, coalescence of the boundary layers attached to the divergent walls is prerequisite to

the development of steady, asymmetric flow in regions outside the boundary layers of the parallel walls.

The charts in figure 13 which refer to the diffuser with  $L/W_1 = 5.50$  and  $R = 2.625$  may appear to preclude extension of this criterion to the regime of unsteady flow. (It has been noted, previously, that the flow in this instance fluctuated violently.) However, the fact that only one of the two successively recorded midheight dynamic-pressure profiles has a maximum ordinate of unity, while the other one falls appreciably short of that value, makes the accuracy of the higher peak somewhat doubtful. Whether or not this suspicion is warranted, it appears that the applicability of the criterion may be extended to include the condition of unsteady flow by stipulating that general asymmetry of discharge will not occur in any exit section (perpendicular to the divergent walls) in which the maximum value of  $q_2/q_{21}$  never falls below unity.

Despite identification of the conditions under which asymmetric flow occurs in two-dimensional diffusers, the origin and mechanism of development of such flows remain conjectural. The prerequisite of boundary-layer coalescence suggests that the dividing layer of air which has not undergone frictional retardation stabilizes the flow by preventing interaction of the shearing forces which characterize the boundary layers. It also appears to the intuition that minute differences between the distributions of velocity and vorticity in the two boundary layers may cause disproportionate asymmetry to develop once the layers come together. These, however, are mere surmises and definite determination of the cause of such asymmetric flow must await further investigation.

Before closing the discussion of this question, attention is drawn to the fact that continuous asymmetric flow is not peculiar to the two-dimensional type of diffuser. Evidence of its occurrence in a conical diffuser has been noted by Persh in the work previously mentioned.

Another general characteristic which received much attention during these experiments was the steadiness of flow. Notes based on visual observations of manometer behavior were made during each test and, although it was expected that they would be of qualitative value only, analysis of these observations enabled the construction, on a chart of  $R$  against  $L/W_1$ , of a reasonably well-defined boundary between the regions of steady and irregular flow.

From the voluminous notes taken during the experiments, the following summary of the information relative to flow steadiness has been prepared.

$L/W_1$	R (steady)	R (fluctuating)
21.75	4.0	5.0
15.25	3.0	4.0
11.00	3.0	3.5
7.75	2.5	3.0
5.50	..... 2.25.....	

Two values of  $R$  are given for all but the shortest diffuser because in that case, only, did one of the test settings appear to coincide with the inception of velocity and pressure fluctuations; in all others the character of flow underwent radical change between consecutive area-ratio settings. The values of  $R$  tabulated above have been plotted in figure 14 and used as a guide for construction of the probable boundary curve. This curve was actually drawn with no guidance but the plotted points. However, when superimposed upon other charts based on accurately determined data, it was found to indicate that irregularity of flow may be expected to occur with a very small increase of divergence angle beyond the value at which the maximum  $C_{PR}$  is attained with a diffuser of fixed length. Further reference to this curve will be made in the discussion of pressure-recovery characteristics.

In addition to those already mentioned, the following miscellaneous flow characteristics are considered noteworthy:

An isolated stream of relatively high velocity and small cross-sectional area persistently penetrated the chaotically turbulent flows in diffusers of large divergence angles. This remnant of continuous flow was highly unstable; it wandered irregularly from top to bottom and from side to side of the exit cross section but, despite these excursions, appeared never to be completely interrupted.

It was found that there was no distinguishable difference as regards the steadiness of flow between long and short diffusers of small area ratio. This is mentioned because the view is known to prevail in some quarters that uniquely steady flow through diffusers of small divergence angle occurs when the boundary layer fills the entire cross section. Only the longer models of the present series fulfilled this condition.

The final item is an interesting side light on the continuous, asymmetric flow observed in long diffusers. The records show that, despite the asymmetry of velocity, the distributions of pressure along the center lines of the divergent walls differed negligibly in the absence of flow separation.

## Pressure-Recovery Characteristics

Since the majority of the results of previous diffuser research have been presented in terms of pressure efficiency, the results of the present investigation will be set forth, initially, in that form.

In figure 15, the experimentally determined values of  $\eta_p$  have been plotted against the corresponding total divergence angles  $2\theta$ . This chart is analogous to the ones used by Gibson to illustrate the primary dependence of diffuser head losses upon divergence angle. While the similarity of the variations of pressure efficiency with divergence angle in diffusers of various length is evident in figure 15, the substantial differences between them clearly indicates that length also influences the value of  $\eta_p$ . In considering this chart, it should be remembered that the value of  $\eta_p$  is not an index of pressure recovery but is merely the ratio of the actual recovery to the ideal one.

When pressure efficiency is plotted as a function of area ratio - as in the upper chart of figure 16 - the effect of length is clearly shown. To be sure, the maximum ordinates of the various curves differ little, but the inferiority of short diffusers in the range of large area ratios and their superiority at small values of  $R$  are quite apparent.

The lower chart of figure 16 illustrates the dependence of the pressure-recovery coefficient  $C_{PR}$  upon both the length and area ratios. Here the predominant influence is that of the length ratio upon the maximum value of  $C_{PR}$ . It can be seen that there is little difference between the pressure-recovery capabilities of diffusers of various lengths when all have small area ratios but it is also apparent that large values of  $C_{PR}$  are attainable only by diffusers of relatively great length. Comparison of the experimental curves with the ideal one<sup>8</sup> brings out the interesting fact that the disparity between experimental and ideal values of  $C_{PR}$  increases with area ratio. It is also worth noting that the curves of  $\eta_p$  and  $C_{PR}$  demonstrate that diffusers of all length ratios attain their maximum  $C_{PR}$  at area ratios considerably larger than those which correspond to maximum  $\eta_p$ . The reason for this disparity was brought out in the comments on equation (15).

While the pressure-recovery characteristics of the tested diffusers are completely defined by figure 16 - in fact, even by figure 15 - alternative forms of graphical representation which greatly facilitate

---

<sup>8</sup>Defined by equation (10).

interpretation of the test results will be found in figures 17 and 18. In the former, contours of  $\eta_p = \text{Constant}$  and, in the latter, contours of  $C_{PR} = \text{Constant}$  have been constructed on a chart having the coordinates  $R$  against  $L/W_1$ . Since the magnitude of the divergence angle is fixed by the values of  $R$  and  $L/W_1$ , that is

$$\theta \approx \arcsin \left( \frac{R - 1}{2L/W_1} \right) \quad (24)$$

auxiliary lines of  $2\theta = \text{Constant}$ <sup>9</sup> also appear on each chart.

Inspection of figure 17 reveals that diffusers of all length ratios attain their maximum pressure efficiencies when the total divergence angle is between  $6^\circ$  and  $7^\circ$ . It will also be seen that the maximum value of  $\eta_p$  diminishes slightly as that of  $L/W_1$  increases. However, aside from the indication that pressure efficiency is closely related to divergence angle, this chart directly conveys little further information of significance because it defines pressure recovery only in relative terms.

In figure 18, the pressure-recovery coefficient is depicted as a function of the length and area ratios. There it will be seen that the divergence angles at which maximum  $C_{PR}$  is attained with diffusers of fixed length ratios are considerably larger than those which yield maximum values of  $\eta_p$  - that is,  $C_{PR}$  is maximum when the value of  $2\theta$  lies between  $9^\circ$  and  $12^\circ$  - and it appears that diffusers shorter than those tested would be characterized by even larger optimum angles. Perhaps the most important fact illustrated by this chart, in conjunction with figure 17, is that, although higher pressure efficiencies are attainable with small values of  $L/W_1$  than with large ones, large values of  $C_{PR}$  can be obtained only by use of relatively long diffusers characterized by large values of  $R$ .

Another matter clarified by figure 18 is the inconsequential effect produced, under certain conditions, by the variation of  $L/W_1$  while  $R$  remains constant. It appears that so long as  $2\theta$  does not exceed the values at which the  $C_{PR}$  contour turns sharply upward,  $L/W_1$  may be reduced without adverse effect. In fact, a slight improvement in the

---

<sup>9</sup>Not rigorously correct because equation (24) implies use of pivot in place of flexure hinge; however, errors are too small to be shown in chart.



value of  $C_{PR}$  at intermediate lengths is indicated by the forms of most of the contours. While considerable latitude in design is thus indicated, it should not be overlooked that an excessive reduction of  $L/W_1$ , while  $R$  remains fixed, will result in drastic reduction of the pressure-recovery coefficient.

It will be of interest to note that the ideal "contours" of  $C_{PR}$  would be horizontal straight lines because the value of  $C_{PRi}$  depends only upon that of  $R$ . (The values of  $C_{PRi}$  which correspond to integral values of  $R$  are shown along the right-hand edge of fig. 18). This fact makes it possible to deduce certain qualitative characteristics of the flow through the diffusers from the shapes of the pressure-recovery contours.

For example, if, in a diffuser of fixed entrance area, the length and area ratios ( $L/W_1$  and  $R$ ) were simultaneously varied in such fashion as to maintain  $C_{PR}$  at a constant value while the divergence angle increased continuously, one of the contours of figure 18 would be traced from right to left along its nearly horizontal segment, then around the vertex, and, finally, along its rising oblique segment. During this hypothetical process, the variation of the exit area  $A_2$  is defined by that of  $R$  (since  $A_1$  is fixed) while the maintenance of  $C_{PR}$  at a constant value implies that  $R_e$  and, therefore, the effective exit area  $A_{2e}$  must remain unchanged in accordance with previous interpretation of the diagrams of figure 12. The difference between the actual and effective areas  $A_2$  and  $A_{2e}$  is, therefore, equal to the area of the actual exit cross section occupied by the idealized boundary layer of displacement thickness. The magnitude of this effective reduction of exit area by the presence of the boundary layer is therefore indicated by the height of the experimentally determined contour of  $C_{PR} = \text{Constant}$  above the corresponding ideal "contour," that is, horizontal line.

By use of these concepts, it is readily deduced that the mean displacement thickness of the exit boundary layer changes inconsequentially as the diffuser length is reduced during the tracing of the substantially horizontal segment of the contour - because  $R$  and, therefore,  $A_2$  vary negligibly. The sharp upturn of the contour toward the vertex, however, indicates that a corresponding increase of displacement thickness must occur as this part of the contour is traced and it is evident that great additional thickening will ensue as the remainder of the contour is traced.

From the foregoing facts concerning the indication of exit boundary-layer displacement thickness by the form of a particular contour of

$C_{PR}$  = Constant, the relative thicknesses of the layers associated with consecutive contours can now be deduced. For example, the fact that the oblique segment of the contour designated 0.74 lies above that of the one designated 0.76 at the abscissa  $L/W_1 = 10$  indicates that the corresponding increase of  $R$  from approximately 3.25 to 3.40, with  $L/W_1 = 10$ , will result in a considerable increase of boundary-layer displacement thickness at the diffuser exit.<sup>10</sup> It thus becomes evident that the rounded vertices of the experimentally determined contours identify the values of  $R$  and  $L/W_1$  at which rapid thickening of the wall boundary layers will begin if the divergence angle of a diffuser of such proportions is further enlarged.

The validity of this analysis appears to be neatly confirmed by the results of the observations of flow steadiness first presented in figure 14. The steady-flow boundary from that chart has been reproduced in figure 18 where it will be seen to lie just above the vertices of the pressure-recovery contours and this orientation is obviously consistent with the fact that intermittent separation and unsteady flow usually ensue when rapid thickening of a boundary layer occurs in the presence of an adverse pressure gradient. The results thus show that, as the divergence angle of a fixed-length diffuser is increased, the pressure efficiency increases to a maximum and diminishes somewhat before the maximum value of the pressure-recovery coefficient is attained. It also appears that attainment of the latter maximum coincides with the inception of separation and unsteady flow.

While no previous work on two-dimensional diffusers is strictly comparable with that reported herein, it may be of interest to see how the present results differ from those of the only other comprehensive work in this field. To enable convenient appraisal of these differences, the comparable portions of Gibson's test data (reference 2) have been transformed into contour charts similar to figures 17 and 18 and these are reproduced as figures 19 and 20.

In figure 19, it will be seen that, although the maximum pressure efficiencies of Gibson's models differ but little from those obtained at equal values of  $L/W_1$  in the present tests, they occur at a divergence angle of approximately  $9^\circ$  - rather than at  $6^\circ$  to  $7^\circ$ , as in the present case. It seems worth noting, also, that the discrepancies between corresponding efficiency contours of figures 17 and 19 diminish markedly as the divergence angle increases to large values.

---

<sup>10</sup>As the ideal "contour" of  $C_{PRi} = 0.74$  lies slightly below that of  $C_{PRi} = 0.76$ , the vertical distance between ideal and actual contours is increased by a little more than the distance between the actual ones designated 0.74 and 0.76.

While the differences between figures 18 and 20 are even more obvious, it will be found that the vertices of the two sets of  $C_{PR}$  contours have almost identical loci, that is, both are curves which lie between the lines  $2\theta = 9^\circ$  and  $2\theta = 12^\circ$ . In most other respects, the two sets of contours differ considerably. The lower segments of those defined by Gibson's results are far from horizontal and, although approximate coincidence will be found at  $C_{PR} = 0.84$ , Gibson's contours for smaller values of  $C_{PR}$  are, in general, displaced toward the left with respect to the corresponding ones of figure 18.

It seems pointless to undertake detailed analysis of these differences because the cross sections of the two families of diffusers had such dissimilar proportions. However, readers who find it difficult to rationalize some of the discrepancies are reminded that Gibson's "exit pressures" were actually measured in an exit duct and are, therefore, larger than would have been the case had the same diffusers discharged into a plenum chamber and the exit pressures been measured there.

The foregoing discussion of pressure recovery has been restricted to consideration of the total increase of static pressure within the diffuser. However, the distributions of pressure along the diverging walls of all the diffusers were also determined and consideration will now be given to those results.

Two typical examples of the variation of wall pressure from entrance to exit are illustrated by figures 21(a) and 21(b); figure 21(b) depicts conditions in undetached flow, whereas evidence of separation is obvious in figure 21(a). (The substantial equality of the pressures at corresponding points of opposite divergent walls illustrated by figure 21(a) is noteworthy because the exit velocity profiles were markedly asymmetric in this case.) While all of the wall pressure data might be similarly presented, this would require a large number of charts and certain desirable comparisons would be rendered inconvenient. For these reasons, another type of chart is used for this purpose.

It consists in a logarithmic plot of the local pressure coefficient against the local area ratio. The special virtue of this chart arises from the relationship between the ideal local pressure coefficient and the local area ratio; by analogy with equation (10) this is

$$C_{\Delta p_i} = 1 - C_{PR_i} = 1 - \left(1 - \frac{1}{r^2}\right) = \frac{1}{r^2} \quad (25)$$

A plot of  $\log C_{\Delta p_i}$  against  $\log r$  therefore takes the form of a straight line through the point (1,1). To make the slope of this line -1,

the modulus of the abscissa scale has been made twice that of the ordinate scale in figures 22(a) to 22(e) which depict the wall pressure distributions in the plain diffusers. Each of these charts refers to diffusers of a single length and various area ratios.

While the curves in all five charts are generally similar in form, detailed examination reveals some significant features. First, it will be noticed that in all cases the disparity between ideal and measured pressures increases with  $r$ , that is, with distance of the point of pressure measurement from the diffuser entrance. This, of course, merely indicates the progressive thickening of the wall boundary layers. However, the approximate coincidence of two or three of the curves of each group indicates that, at least within certain ranges of the divergence angle or longitudinal pressure gradient, the wall pressures are controlled almost exclusively by cross-sectional area and are negligibly influenced by distance from the entrance.

If this apparent relationship is not fortuitous, it should be substantiated by the positions of the closely grouped curves in all five charts, that is, by the data for diffusers of all lengths. Comparison of the ordinates of the lowest curves in each chart at several values of  $r$  shows that they do, indeed, differ by extremely small amounts. It thus appears that in the best<sup>11</sup> diffusers of various lengths the pressure coefficients for cross sections of equal area differ negligibly. Attention is called to the fact that this finding is consistent with the previously noted negligible effect of length upon the values of  $C_{pr}$  for diffusers of fixed area ratio and less-than-optimum divergence. It should be added that this finding is not without precedent and that previously reported data on boundary-layer growth give evidence of its applicability to certain conical diffusers; this will be found in reference 18 on page 21 and in figure 13.

The probable reasons for the departure of some of the curves in each chart from the group of nearly coincident ones will be examined next. Since the discrepancy between actual and ideal pressures is a consequence of the presence of a retarded boundary layer in the actual flow, these "nonconforming" pressure curves must result from the presence of unusually thick boundary layers in the diffusers to which they correspond. Excessive thickness is, of course, to be expected when the divergence angle and adverse pressure gradient become so large that flow separation occurs and this would appear to be an adequate explanation of the upward displacement of the pressure curves for the larger area ratios (and divergence angles) in each chart.

---

<sup>11</sup>"Best" is used to denote the diffuser having the smallest value of  $C_{\Delta p}$  at a given value of  $r$ .

On the other hand, it will be noted that the pressure curves for  $R = 2$  lie above those for  $R = 3$  and  $R = 4$  in the charts for  $L/W_1 = 21.75$  and  $15.25$  and that this inconsistency disappears as the length is reduced. It is obvious that the foregoing explanation is invalid in this case for there is no reason to believe that the boundary-layer displacement thickness is greater when  $R = 2$  than when  $R = 3$ . However, it does appear both possible and probable that the ratio of displacement thickness to channel width may cease to diminish, and actually increase, as the longitudinal pressure gradient falls to the very low values which characterize the long diffusers in question. While experimental evidence to substantiate this tentative explanation is wanting, the nonconformity of these pressure curves for long diffusers of small area ratio shows that the range of validity of the pressure-area relationship discussed above is not only limited on one hand by the appearance of separated flow but on the other by factors as yet undetermined but probably definable in terms of minimum adverse pressure gradient.

At this point, cognizance must be given to the possible misconception that failure to include total-pressure-loss data compromises the usefulness of the results. To spare readers this misconception, it is noted that these data were intentionally omitted because, as is explained below, they convey no useful information about diffusers which discharge into plenum chambers and are inapplicable to any other exit condition.

Aside from facilitating description of the outflow from a diffuser, the only value of exit survey data is that they may enable appraisal of the total pressure available for subsequent compression or acceleration of the discharged fluid. However, when a diffuser discharges into a large plenum chamber - as in these experiments - the total pressure available for such purposes is identical with the static pressure in the plenum chamber, where the velocity is negligible. Therefore, information regarding the loss of total pressure within the diffuser is superfluous when the plenum-chamber pressure is known - as is the case herein - and, in fact, it does not even enable calculation of the plenum-chamber pressure unless the distribution of exit velocity is also known.

The other reason for the omission was the author's fear that such data, if presented, would be misused in attempts to predict the performance of similar diffusers which discharge into ducts. The fact that the addition of even a short length of uniform-section discharge duct substantially modifies the performance of a given diffuser<sup>12</sup> indicates the inapplicability to other exit conditions of total-pressure-loss data derived from tests which involved plenum-chamber discharge.

---

<sup>12</sup>See discussion of diffusers with parallel-wall exit sections under "Effects of Modifications."

It seems worth adding that flow instability made it practically impossible to obtain dependable exit survey data for diffusers characterized by divergence angles greater than those at which maximum  $C_{PR}$  occurs. Since proof of this fact by "continuity checks" invalidated a large part of the exit survey data, omission of the remainder appears not only warranted but wise.

### Volumetric Efficiency and Effective Area Ratio

In frictionless flow through a diffuser of area ratio  $R$ , the uniform entrance and exit velocities are, of course, inversely proportional to the corresponding areas, whence

$$V_{1i}/V_{2i} = R \quad (26)$$

Under actual conditions of viscous flow, continuity requires that the mean velocities be similarly related, that is,

$$\bar{V}_1/\bar{V}_2 = R \quad (27)$$

However, since  $\bar{V}_2 < V_{2i}$ , the actual entrance velocity and, therefore, the volumetric flow rate fall short of the ideal quantities -

$$\bar{V}_1 < V_{1i}$$

$$Q < Q_i$$

and the volumetric efficiency

$$\eta_v = \frac{Q}{Q_i} = \frac{R_e}{R} = \frac{1}{R\sqrt{1 - C_{PR}}} \quad (28)$$

is always less than unity.

In figure 23, the volumetric-efficiency characteristics of the plain diffusers are presented in the form of a contour chart. It will be seen that this chart has little resemblance to the analogous pressure-efficiency diagram, figure 17. Volumetric efficiency diminishes steadily as area ratio increases and the rate of reduction is greater at small values of  $L/W_1$  than at large ones. A significant consequence of this

nonuniformity is that much higher volumetric efficiency is attainable at small values of the pressure-recovery coefficient than at large ones. In fact, the results indicate that high volumetric efficiency and large values of  $C_{PR}$  are simply irreconcilable in diffusers of the type tested.<sup>13</sup>

This anomaly arises from the relative positions of the contours of  $\eta_v = \text{Constant}$  and  $C_{PR} = \text{Constant}$ . Segments of two typical contours, those for  $C_{PR} = 0.70$  and  $0.84$  (from fig. 18) have been superimposed upon the volumetric-efficiency chart, figure 23. It will be seen that, when  $L/W_1 = 6.0$  and  $C_{PR} = 0.70$ ,  $\eta_v = 0.80$  and that, when  $L/W_1 = 21.7$  and  $C_{PR} = 0.84$ ,  $\eta_v = 0.575$ . Thus, the volumetric efficiencies of the shortest diffusers capable of developing pressure-recovery coefficients of  $0.70$  and  $0.84$  are  $0.80$  and  $0.575$ , respectively. The practical implication of these efficiencies and their disparity is that in order to provide specified volumetric air-flow rates in diffusers of the proportions cited above their cross-section areas would have to be made 25 and 74 percent larger, respectively, than those which would suffice if ideal exit velocities prevailed at all points of their exit cross sections, that is,  $1/0.80 = 1.25$  and  $1/0.575 = 1.74$ .

The fact that the effective area ratio of a diffuser is alternatively definable in terms of either the pressure-recovery coefficient or the volumetric efficiency and geometric area ratio, that is,

$$R_e = \eta_v R = 1/\sqrt{1 - C_{PR}} \quad (29)$$

affords a means of portraying, in a single diagram, the effects of the basic design variables ( $R$  and  $L/W_1$ ) upon both the pressure-recovery and volumetric-efficiency characteristics of a family of diffusers. This fact has been utilized for the preparation of figure 24 wherein contours of  $R_e = \text{Constant}$ , derived from the data in table II, are shown on a chart of  $R$  against  $L/W_1$ .

A typical contour, for example, the one designated  $R_e = 2.0$ , identifies the proportions ( $R$  and  $L/W_1$ ) of all the diffusers - within the scope of these tests - which have the same performance characteristics as an ideal diffuser of  $R = 2.0$ . All of the diffusers so identified are characterized by the pressure-recovery coefficient

$$C_{PR} = 1 - \frac{1}{R_e^2} = 1 - \frac{1}{4} = 0.75 \quad (30)$$

---

<sup>13</sup>This appears to be true, to a considerable degree, of all types of diffusers in which the boundary layer is not controlled.

and the mean entrance velocity is, in every case, exactly twice the ideal discharge velocity, that is,

$$\bar{V}_1 = 2V_{2i} = 2\sqrt{2\Delta p_2/\rho} \quad (31)$$

The widely varied diffuser proportions which yield identical performance characteristics are indicated, for this particular case, by the following typical sets of values:

R	L/W <sub>1</sub>	2θ (deg)	Re	C <sub>PR</sub>
2.5	17.0	5.0	2.0	0.75
2.6	8.3	11.1	2.0	.75
3.5	10.4	13.5	2.0	.75
5.0	15.3	15.0	2.0	.75

Inspection of the contours in figure 24 will reveal that the differences between R and Re may be relatively small when R is small (as a consequence of high volumetric efficiencies attainable under that condition) but that the minimum discrepancies, both relative and absolute, increase as R is enlarged. It is interesting to notice that the largest value of Re attained within the scope of these tests was 2.5. The attainment of this value by a diffuser with an area ratio of 4.35 and a length of 21.7W<sub>1</sub> may serve to emphasize the extent to which the actual performance characteristics of two-dimensional diffusers fall short of the corresponding ideal ones under the conditions necessary for the realization of large values of the pressure-recovery coefficient.

#### Effects of Modifications

Asymmetry.- Tests of asymmetric diffusers were made in an effort to separate the effects of divergence angle from those of longitudinal pressure gradient.

As may be seen in figure 25, it was found that the pressure recovery effected by an asymmetric diffuser differed imperceptibly from that of a comparable symmetric one so long as the area ratio did not exceed that at which the latter attained a maximum value of C<sub>PR</sub>. With greater-than-optimum area ratios, asymmetric diffusers proved inferior to symmetric ones.

These results prove beyond all reasonable doubt that flow separation in plane-wall, two-dimensional diffusers is not the consequence of a mere change of flow direction of certain magnitude. On the contrary,



the attainment by both types of equal maximum values of  $C_{PR}$  at equal values of  $R$  unmistakably identifies longitudinal pressure gradient as the factor of predominant influence upon flow separation.

Diffusers with parallel-wall exit sections.- Tests of symmetrical models with parallel-wall terminal sections were made, primarily, to determine the effects of incorporating such exit sections in diffusers of fixed area ratio and over-all length and, incidentally, to verify by observations of wall pressure distribution the previously reported increase of static pressure in the uniform discharge passage.

The pressure-recovery characteristics of symmetrical diffusers of  $R = 2$  and  $3.5$  which had parallel walls extending from  $L/W_1 = 11.00$  to  $L/W_1 = 15.25$  are compared in figure 26 with those of continuously divergent diffusers of the same area ratios but with  $L/W_1 = 11.00$  as well as  $L/W_1 = 15.25$ . From the curves it is evident that the addition of even a short, uniform duct to a diffuser of  $L/W_1 = 11.00$  slightly augments both the maximum value of the pressure-recovery coefficient and the area ratio at which it occurs. It will also be seen that somewhat larger improvements of  $C_{PR}$  are obtained at greater-than-optimum values of  $R$  and that minor improvement is obtained even when  $R$  is relatively small. On the other hand, it is apparent that the discontinuous form is inferior to a continuously divergent one of equal length ( $L/W_1 = 15.25$ ) at all but small values of  $R$ .

The results of the wall pressure observation shown in figure 27 substantiate the finding that static pressure increases in a straight exit duct despite the uniformity of its cross-sectional area. This, of course, is the source of the improved performance obtained by adding the duct.

The superiority of the continuously divergent diffuser of the same area ratio and over-all length as those of the discontinuous one is undoubtedly due to the difference between the longitudinal pressure gradients which characterize the two types. Since the extended diffuser has the larger divergence angle and pressure gradient, it is to be expected that flow separation and reduction of  $C_{PR}$  will occur at a smaller value of  $R$  in that case than in the other one.

The results of these tests thus indicate that the addition of even a short parallel-wall extension enhances the performance of a given plane-wall, two-dimensional diffuser. However, they also show that the incorporation of such a uniform section in a diffuser of fixed area ratio and limited over-all length - with consequent increase of divergence

angle and longitudinal pressure gradient - results in negligible improvement if the area ratio is small and has an adverse effect if it is large.

Diffusers with central partition.- When a thin, central partition is installed in a given two-dimensional diffuser, the two asymmetric diffusers so formed have the same area ratio as the original one but the length ratio  $L/W_1$  is doubled by the halving of  $W_1$ . Since the effect of asymmetry has been shown to be negligible so long as the area ratio is less than the optimum value for a comparable symmetric diffuser, such modification would appear to afford a means of substantially duplicating the pressure-recovery capabilities of long diffusers in short ones. Exploration of the practical possibilities of so improving the performance of relatively short diffusers was therefore included in the present program.

In the previous description of the models used for this purpose, it was mentioned that instability of the thin partition necessitated the installation of lateral supports. The wakes of those at the leading edge of the partition undoubtedly caused the flow to differ markedly, and probably very adversely, from that which would have prevailed with an unrestrained, but stable, partition. However, even under these unfavorable conditions, a sufficient improvement of performance was obtained to warrant its discussion herein.

The pressure-recovery characteristics of plain and divided diffusers with  $L/W_1 = 7.75$  are shown in figure 28. Four features of the latter warrant individual attention. In order of diminishing importance they are: The attainment of a maximum value of  $C_{PR}$  at  $R = 3$  (instead of  $R = 2.5$ , as in the case of the undivided diffuser), the attainment of a maximum value of  $C_{PR}$  greater than that for the plain diffuser, the marked superiority of the divided type when  $R \geq 3.0$ , and its inferiority when  $R \leq 2.6$ .

The fact that the pressure-recovery coefficient continues to increase until  $R = 3.0$  is interpreted as evidence that substantial flow separation is suppressed until that value is attained. Reference to figure 16 will show that a length ratio of 11 is required to achieve the same result with an undivided, symmetrical diffuser. Insofar as flow separation is concerned, the partitioning of the diffuser is approximately equivalent to an increase of  $L/W_1$  from 7.75 to 11.

While further comparison of figures 16 and 28 shows that the maximum pressure-recovery coefficient obtained with the divided diffusers is appreciably smaller than that for plain ones with  $L/W_1 = 11.00$ , it is believed that this deficiency is largely, if not entirely, the result of the dissipation of energy in the wakes of the lateral supports which, it will be remembered, were bars of unfaired, rectangular section.

These two features of the results thus indicate that the partitioning of a diffuser of  $L/W_1 = 7.75$  increases the optimum area ratio from 2.5 to 3.0 - thereby making the flow separation effectiveness that of a plain diffuser with  $L/W_1 = 11.00$  - and that the maximum value of  $C_{PR}$ , which actually increased only from 0.741 to 0.755, would be much more substantially improved if the parasitic supporting members could be eliminated. It is also noted that the effective area ratio of the divided diffuser of  $R = 3.0$  is 2.016, whereas table II shows that the largest value of  $R_e$  attained by plain diffusers of  $L/W_1 = 7.75$  is only 1.965.

The significance of the improvement of pressure recovery at values of  $R$  greater than 3.0 is believed to be more apparent than real. Although previous experimenters have expressed the view that augmentation of the pressure efficiency or pressure recovery in diffusers of greater-than-optimum divergence is an improvement of considerable practical value "when allowable dimensions are limited," this implies that the primary function of a diffuser is the reduction of velocity and that pressure recovery is of secondary importance. Ordinarily, however, the reverse is true, that is, the transformation of dynamic into static pressure is the principal function of a diffuser and, under this condition, there is no justification for using one which incorporates greater-than-optimum divergence. Improvement of the performance of diffusers of fixed length ratio  $L/W_1$  under the conditions of ordinary use is therefore demonstrable only by increase of the maximum value of  $C_{PR}$  and the augmentation of  $C_{PR}$  at area ratios larger than the optimum one is significant only as regards applications in which velocity reduction is of greater importance than pressure recovery.

The fact that introduction of the partition reduced the pressure-recovery coefficients for area ratios less than the optimum value for the undivided diffuser is neither surprising nor consequential. This reduction of  $C_{PR}$  is, of course, the result of the additional frictional losses arising from the retardation of the air in the boundary layers of the central partition. However, since flow separation does not occur in plain diffusers at the area ratios under consideration, the installation of a partition under such conditions serves no useful purpose and its effects are, therefore, inconsequential.

The results of these experiments on partitions are considered unsatisfactory because they are inconclusive. Appraisal of the modest improvements actually effected is complicated by the unknown effects of the parasitic structure. Nevertheless, the fact that appreciable improvement was demonstrated under the unfavorable conditions which prevailed proves that the central partition has some merit and would appear to justify further investigation of the potentialities of internally subdividing short, wide-angle diffusers.

Diffusers with central wedge.- In an effort to secure the benefits of centrally dividing a short, wide-angle diffuser and at the same time avoid the necessity of providing lateral restraints for the dividing member, a self-supporting wedge of small included angle was substituted for the previously tested plate partition. Tests of this arrangement produced disappointing results and, although the cause became apparent before the experiments were finished, time did not permit its rectification. However, some facts of considerable interest were revealed by the data and comments upon them appear below.

The pressure-recovery characteristics determined with the wedge in place differ very slightly from those which characterize plain diffusers of equal length and area ratios. Unfavorably as this compares with the general performance of the thin plate partition, one favorable feature is disclosed by the data for  $R = 2.5$ , the area ratio which marks the peak of the curve of  $C_{PR}$  against  $R$  for the comparable plain diffusers (see fig. 29); it is the very small difference between the ordinates of the two curves at that abscissa.

Two possible explanations for such approximate equality may be advanced. One is that the installation of the wedge causes a very small increase of frictional losses; in view of the approximate doubling of the wetted surfaces, this seems improbable. The other is that an appreciable increase of frictional loss is compensated by the suppression of incipient separation - and this appears the more logical of the two. Whatever the truth may be, comparison of figures 28 and 29 shows that a larger value of  $C_{PR}$  is obtained at  $R = 2.5$  with the wedge than with the externally supported plate partition. This fact lends support to the view that elimination of the external supports would appreciably improve the pressure-recovery characteristics of the latter.

The failure of the wedge to suppress flow separation to any such extent as did the plate was traced to a combined effect of form and location. The truncated leading edge of the wedge was located a short distance downstream from the diffuser entrance with the hastily conceived and erroneous idea that the projected surfaces should intersect in the entrance plane. The unfortunate result of this choice of position is illustrated by figure 30 wherein the curves depict the variations of velocity ratio and pressure-recovery coefficient which would occur in frictionless flow near the leading edge of the wedge when  $R = 3.0$ . It will be seen that the rates of retardation and pressure change between the diffuser entrance and foremost point of the wedge correspond to a diffuser with  $R = 3.83$  and that only farther downstream do they abruptly change to the values appropriate to  $R = 3.0$ . Since tufts indicated that unmistakable separation of flow from the divergent walls occurred opposite the nose of the wedge when  $R = 3.0$ , there seems little doubt that over-rapid initial expansion prevented the wedge from performing its intended function.

## CONCLUSIONS

The following conclusions are drawn from the results of these experiments on plane-wall, two-dimensional diffusers:

1. Satisfactory approximation of two-dimensional flow was obtained at all divergence angles smaller than those characterized by intermittent separation and marked unsteadiness of flow.
2. Steady, unseparated, asymmetric flow appears to occur only when the wall boundary layers coalesce before reaching the diffuser exit.
3. As the divergence angle of a diffuser of fixed length increases, steady flow prevails until the pressure-recovery coefficient attains its maximum value; immediately thereafter, unsteadiness becomes noticeable and the flow then degenerates rapidly into a state of violent pulsation and chaotic turbulence.
4. In diffusers of all the length ratios  $L/W_1$  tested, maximum pressure efficiency  $\eta_p$  occurred when the total divergence angle was between  $6^\circ$  and  $7^\circ$  and the maximum value of  $\eta_p$  ( $L/W_1 = \text{Constant}$ ) declined by only 2 percent as  $L/W_1$  increased from 5.50 to 21.75.
5. Maximum values of the pressure-recovery coefficient  $C_{PR}$  for diffusers of various length ratios occurred at total divergence angles which ranged from about  $12^\circ$  for  $L/W_1 = 5.50$  to  $9^\circ$  for  $L/W_1 = 21.75$ . The corresponding maximum values of  $C_{PR}$ , which were 0.688 and 0.840, respectively, indicate the marked influence of length ratio upon the pressure-recovery capabilities of diffusers.
6. Variation of the length ratio while the area ratio remains constant has a practically negligible effect upon the pressure-recovery coefficient so long as the divergence angle remains appreciably smaller than that at which the maximum value of  $C_{PR}$  is attained at the fixed area ratio. A corollary finding is the negligible effect of length ratio upon the displacement thickness of the exit boundary layer under these conditions.
7. Volumetric efficiency diminishes as area ratio increases and at a rate which diminishes as the length ratio increases. The result of this variation is to preclude simultaneous achievement of high volumetric efficiency and large pressure recovery.
8. The physical significance of experimentally determined diffuser performance characteristics appears to be most clearly illustrated by delineating the effective area ratio as a function of the geometric

length and area ratios. The largest value of effective area ratio attained in these experiments - which included the testing of diffusers having length and area ratios as great as 21.75 and 5.0, respectively - was 2.5.

9. Tests of asymmetric diffusers demonstrated that flow separation is primarily controlled by longitudinal pressure gradient rather than by change of flow direction, or wall divergence angle, per se.

10. Appreciable improvement of pressure recovery results when even a short exit duct of uniform cross section is added to a diffuser.

11. In diffusers of small length ratio, the installation of a thin, central, longitudinal partition augments the maximum pressure-recovery coefficient by suppressing flow separation and increasing the optimum divergence angle.

Stanford University

Stanford, Calif., September 25, 1950

## REFERENCES

1. Gibson, A. H.: On the Flow of Water through Pipes and Passages Having Converging or Diverging Boundaries. Proc. Roy. Soc. (London), ser. A, vol. LXXXIII, no. 563, March 2, 1910, pp. 366-378.
2. Gibson, A. H.: On the Resistance to Flow of Water through Pipes or Passages Having Divergent Boundaries. Trans. Roy. Soc. (Edinburgh), vol. XLVIII, pt. 1, art. no. 5, 1913, pp. 97-116.
3. Patterson, G. N.: Modern Diffuser Design. Aircraft Engineering, vol. 10, no. 115, Sept. 1938, pp. 267-273.
4. Ackeret, J.: Grenzschichtabsaugung. Z.V.D.I., Bd. 70, Nr. 35, Aug. 28, 1926, pp. 1153-1158. (Also available in translation as NACA TM 395, 1926.)
5. Prandtl, L.: Über Flüssigkeitsbewegung bei sehr kleiner Reibung. Verh. dritten Internationalen Mathematikerkongresses (Heidelberg, 1904), Teubner (Leipzig), 1905, pp. 484-491. (Also available in translation as NACA TM 452, 1928.)
6. Schrenk, Oskar: Versuche an einer Kugel mit Grenzschichtabsaugung. Z.F.M., Jahrg, 17, Heft 17, Sept. 14, 1926, pp. 366-372. (Also available in translation as NACA TM 388, 1926.)
7. Biebel, William J.: Low-Pressure Boundary-Layer Control in Diffusers and Bends. NACA WR L-84, 1945. (Formerly NACA ARR L5C24.)
8. Frey, Kurt: Verminderung des Strömungsverlustes in Kanälen durch Leitflächen. Forsch. Geb. Ing.-Wes., Bd. 5, May/June 1934, pp. 105-117.
9. Peters, H.: Energieumsetzung in Querschnittserweiterungen bei verschiedenen Zulaufbedingungen. Ing.-Archiv, Bd. II, Heft 1, March 1931, pp. 92-107. (Also available in translation as NACA TM 737, 1934.)
10. Nikuradse, Johann: Untersuchungen über die Strömungen des Wassers in konvergenten und divergenten Kanälen. Forsch.-Arb. Geb. Ing.-Wes., Heft 289, 1929.
11. Andres, K.: Versuche über die Umsetzung von Wassergeschwindigkeit in Druck. Mitt. Forsch.-Arb. Geb. Ing.-Wes., Heft 76, 1909.

12. Hochschild, Heinrich: Versuche über die Strömungsvorgänge in erweiterten und verengten Kanälen. Mitt. Forsch.-Arb. Geb. Ing.-Wes., Heft 114, 1912.
13. Kröner, Richard: Versuche über Strömungen in stark erweiterten Kanälen. Forsch.-Arb. Geb. Ing.-Wes., Heft 222, 1920.
14. Dönch, Fritz: Divergente und konvergente turbulente Strömungen mit kleinen Öffnungswinkeln. Forsch.-Arb. Geb. Ing.-Wes., Heft 282, 1926.
15. Vedernikoff, A. N.: An Experimental Investigation of the Flow of Air in a Flat Broadening Channel. NACA TM 1059, 1944. (Translation of CAHI Rep. No. 137, 1926.)
16. Demontis, Jean: Recherches sur l'influence de l'angle d'ouverture d'un ajutage divergent sur l'écoulement à deux dimensions de l'air à travers cet ajutage. Pub. sci. et tech. du Ministère de l'air, no. 87, 1936.
17. Polzin, J.: Flow Investigations in a Two-Dimensional Diffuser. R.T.P. Translation No. 1286, British Ministry of Aircraft Production. (Translation from Ing.-Archiv, Bd. 11, Heft 5, Oct. 1940, pp. 361-385.)
18. Robertson, J. M., and Ross, D.: Water Tunnel Diffuser Flow Studies; Part II - Experimental Research. The Penn. State College, July 8, 1949.



TABLE I  
SIDE-PLATE ORIFICE LOCATIONS

[ $l$ , distance of side-plate orifice from diffuser entrance, in.;  $L$ , length of diffuser side plate, in.]

Orifice	$l$ (in.)	$l/W_1$	$L$ (in.)	$L/W_1$
1	2.625	0.656	22.0	5.50
2	3.625	.906		
3	4.625	1.156		
4	5.625	1.406		
5	6.625	1.656		
6	7.625	1.906		
7	8.625	2.156		
8	9.625	2.406		
9	10.625	2.656		
10	12.625	3.156		
11	14.625	3.656		
12	16.625	4.156		
13	18.625	4.656		
14	20.625	5.156		
15	24.625	6.156	31.0	7.75
16	28.625	7.156		
17	32.625	8.156		
18	36.625	9.156	44.0	11.00
19	40.625	10.156		
20	46.625	11.656		
21	52.625	13.156		
22	58.625	14.656	61.0	15.25
23	64.625	16.156		
24	73.625	18.406		
25	82.625	20.656	87.0	21.75



TABLE II  
 PERFORMANCE CHARACTERISTICS OF PLAIN DIFFUSERS  
 (SYMMETRICAL, PLANE-WALL, TWO-DIMENSIONAL TYPE)

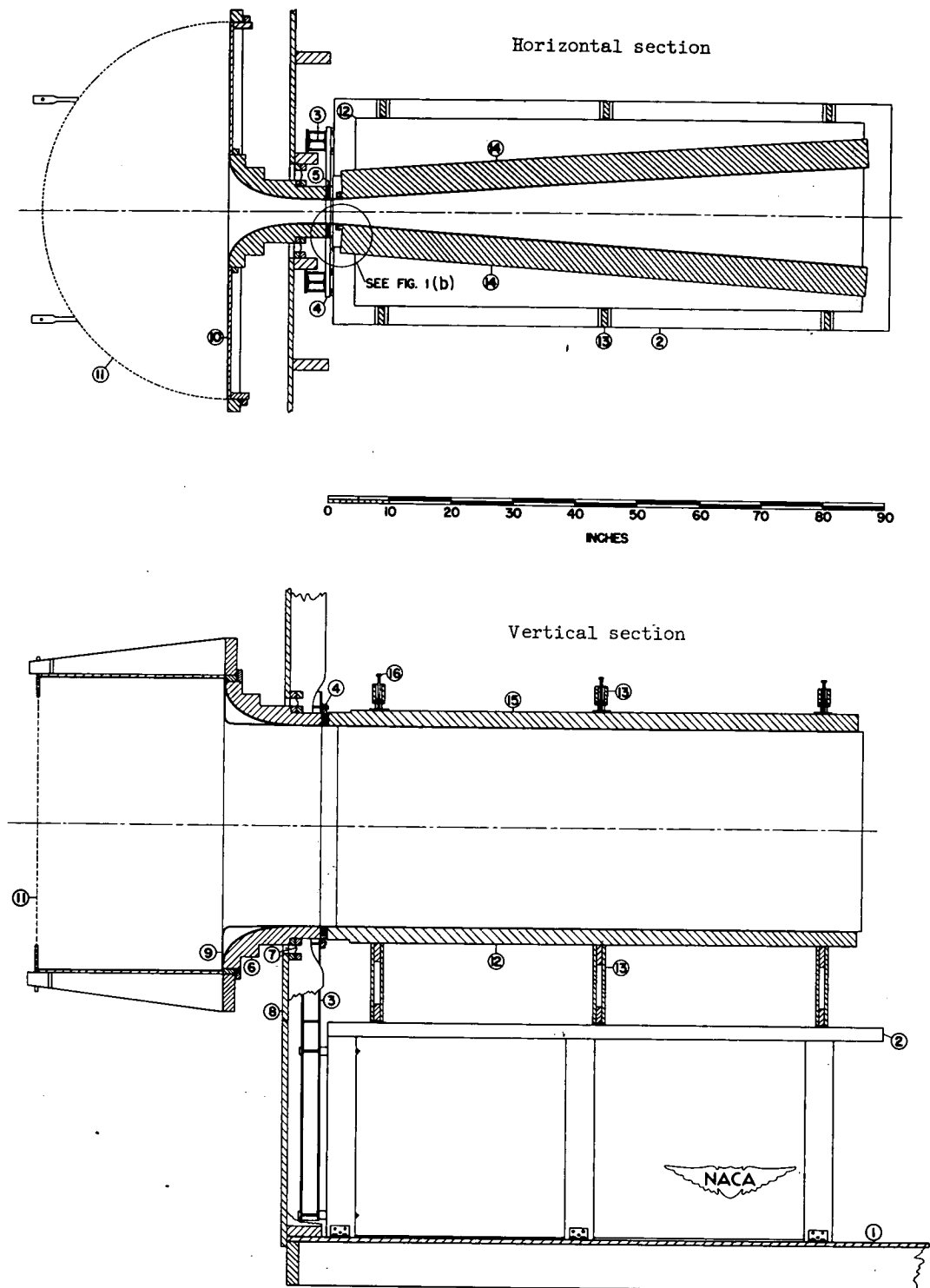
L (in.)	L/W <sub>1</sub>	W <sub>2</sub> (in.)	R	2θ (deg)	C <sub>PR</sub>	Re	η <sub>p</sub>	η <sub>v</sub>
87	21.75	8.0	2.0	2.67	0.650	1.689	0.866	0.845
		12.0	3.0	5.37	.796	2.214	.896	.738
		16.0	4.0	8.03	.838	2.485	.894	.621
		20.0	5.0	10.70	.836	2.469	.871	.494
61	15.25	8.0	2.0	3.80	.667	1.738	.889	.869
		12.0	3.0	7.60	.799	2.231	.899	.744
		16.0	4.0	11.40	.813	2.312	.868	.578
		20.0	5.0	15.20	.748	1.992	.780	.398
44	11.00	8.0	2.0	5.38	.676	1.756	.904	.878
		10.0	2.5	7.92	.756	2.025	.901	.810
		12.0	3.0	10.58	.788	2.171	.886	.727
		14.0	3.5	13.20	.766	2.068	.833	.591
		16.0	4.0	15.88	.714	1.869	.762	.467
31	7.75	7.2	1.8	6.02	.635	1.655	.919	.920
		8.0	2.0	7.53	.684	1.779	.914	.889
		10.0	2.5	11.30	.741	1.965	.882	.786
		12.0	3.0	15.10	.710	1.866	.799	.662
		14.0	3.5	18.90	.644	1.676	.701	.479
22	5.50	7.0	1.75	8.02	.619	1.620	.918	.832
		8.0	2.00	10.72	.671	1.744	.897	.872
		9.0	2.25	13.38	.688	1.790	.857	.796
		10.5	2.625	17.43	.619	1.620	.725	.617



TABLE III  
PERFORMANCE CHARACTERISTICS OF MODIFIED DIFFUSERS

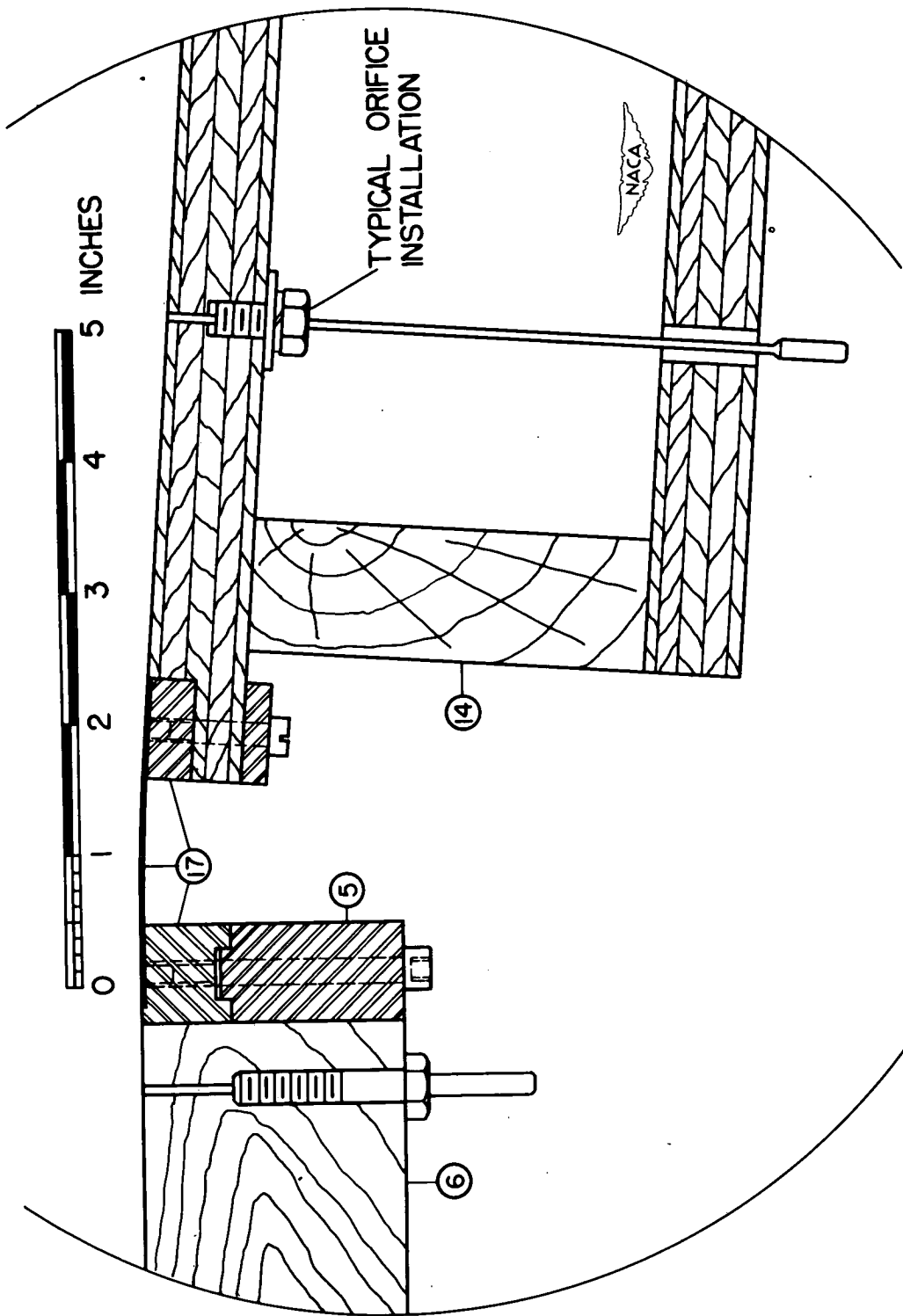
L (in.)	L/W <sub>1</sub>	W <sub>2</sub> (in.)	R	2θ (deg)	C <sub>PR</sub>	R <sub>e</sub>	η <sub>p</sub>	η <sub>v</sub>
Asymmetric diffusers - one straight and one divergent wall								
31	7.75	8.0	2.0	7.57	0.688	1.790	0.917	0.895
		10.0	2.5	11.36	.744	1.976	.886	.790
		12.0	3.0	15.22	.675	1.753	.759	.584
Extended diffusers - parallel walls from L/W <sub>1</sub> = 11.00 to L/W <sub>1</sub> = 15.25								
<sup>a</sup> 61	15.25	8.0 14.0	2.0 3.5	<sup>b</sup> 5.38 <sup>b</sup> 13.20	0.684 .793	1.778 2.198	0.912 .864	0.889 .628
Diffusers with central partition - partition thickness, 0.125 in.								
31	<sup>c</sup> 7.75	<sup>c</sup> 10.0	<sup>c</sup> 2.5	11.30	0.726	1.910	0.864	0.764
		<sup>c</sup> 12.0	<sup>c</sup> 3.0	15.10	.754	2.016	.849	.672
		<sup>c</sup> 14.0	<sup>c</sup> 3.5	18.90	.728	1.916	.792	.547
Diffusers with central wedge - wedge included angle, 3.30°								
31	7.75	<sup>d</sup> 10.0	2.5	<sup>e</sup> 11.13	0.735	1.942	0.875	0.777
		<sup>d</sup> 12.0	3.0	<sup>e</sup> 15.15	.716	1.876	.800	.625

<sup>a</sup>Over-all length.<sup>b</sup>Divergent section only.<sup>c</sup>Without correction for thickness of partition.<sup>d</sup>Total width of open passages.<sup>e</sup>2(θ - Ω), deg.



(a) Longitudinal sectional views.

Figure 1.- Diffuser test installation.



(b) Hinge details.

Figure 1.- Concluded.

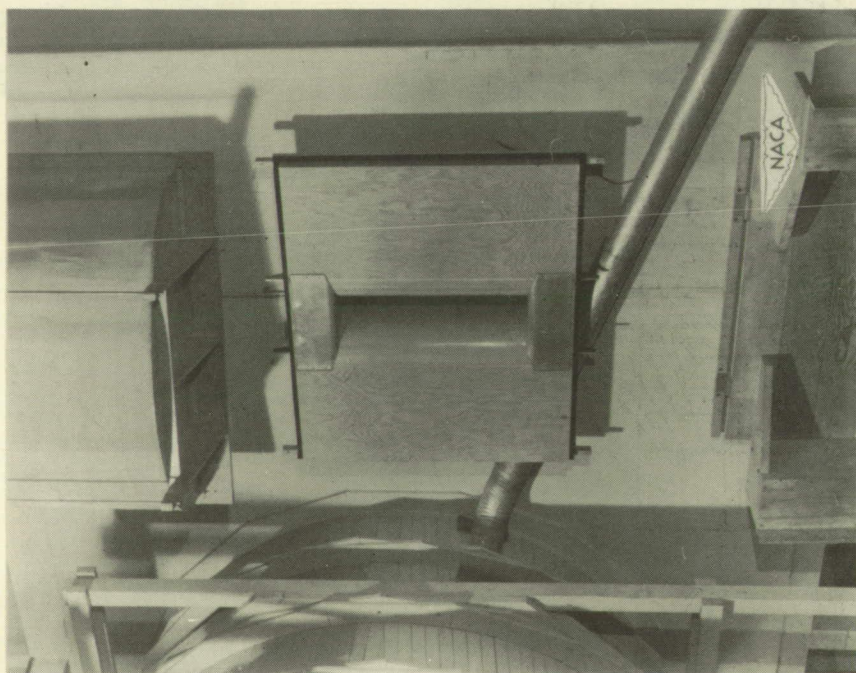


Figure 2.- Bellmouth and plate  
with screen elevated.

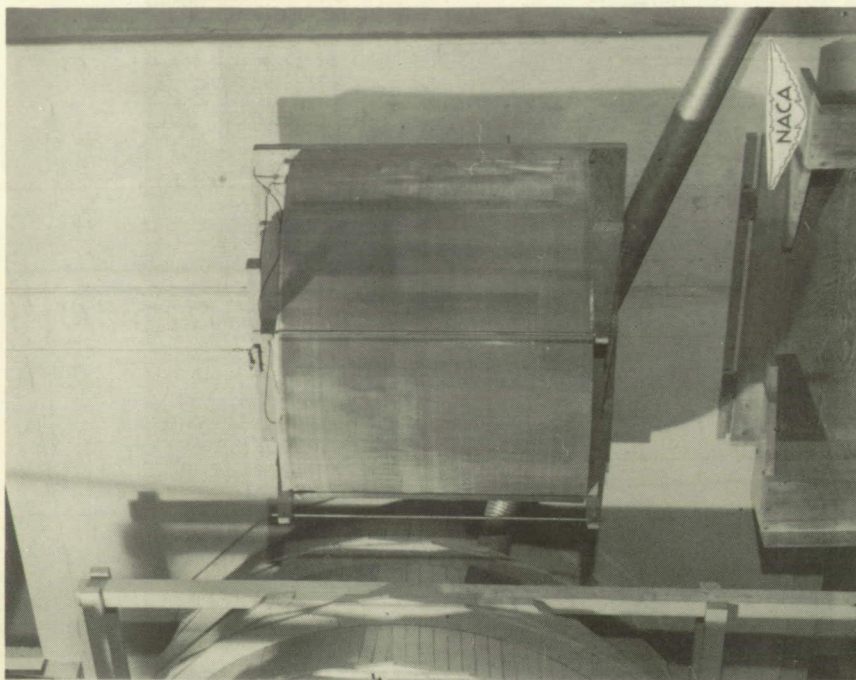


Figure 3.- Entrance with screen  
in operating position.



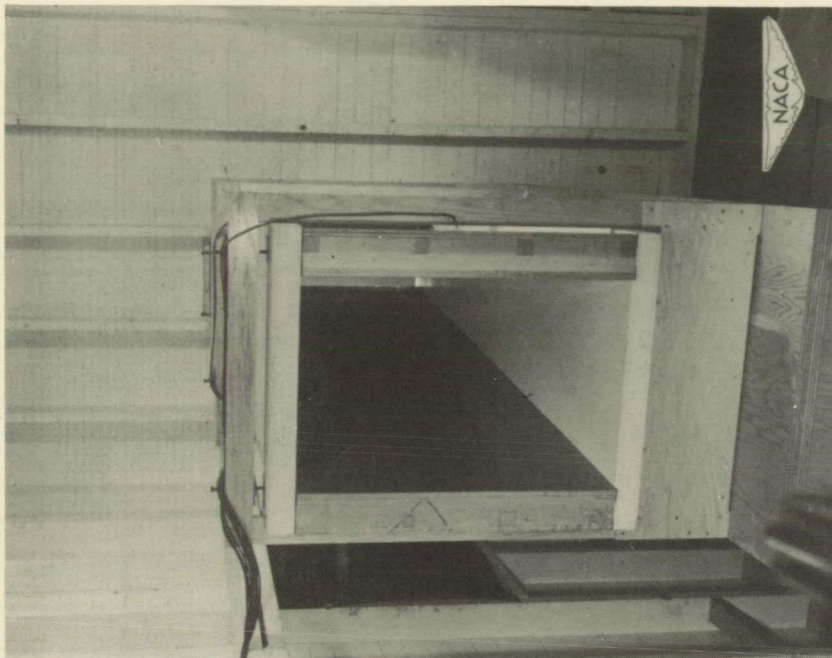


Figure 5.- Plain diffuser.  
 $L/W_1 = 21.75$ ;  $R = 5.0$ .

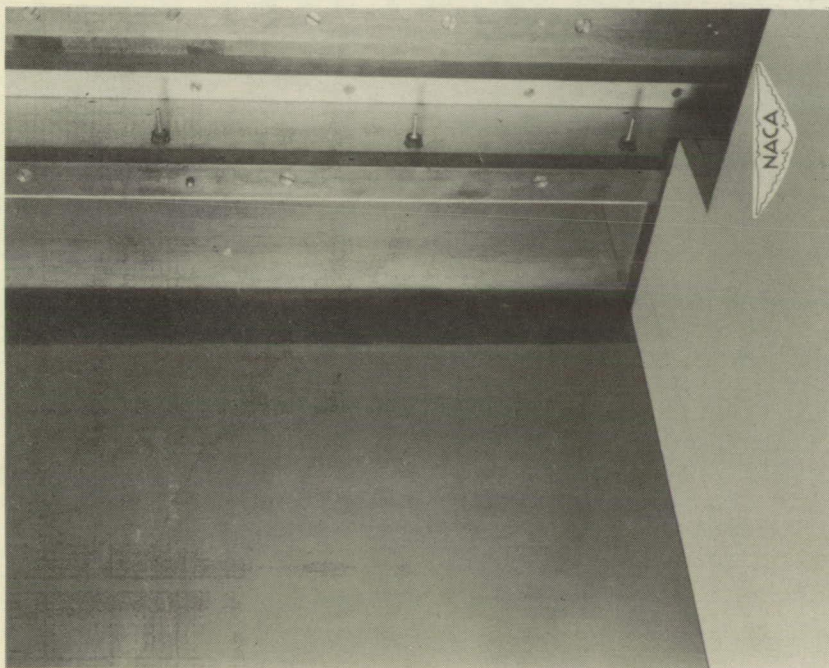


Figure 4.- Details of bellmouth,  
 hinge, and plates.

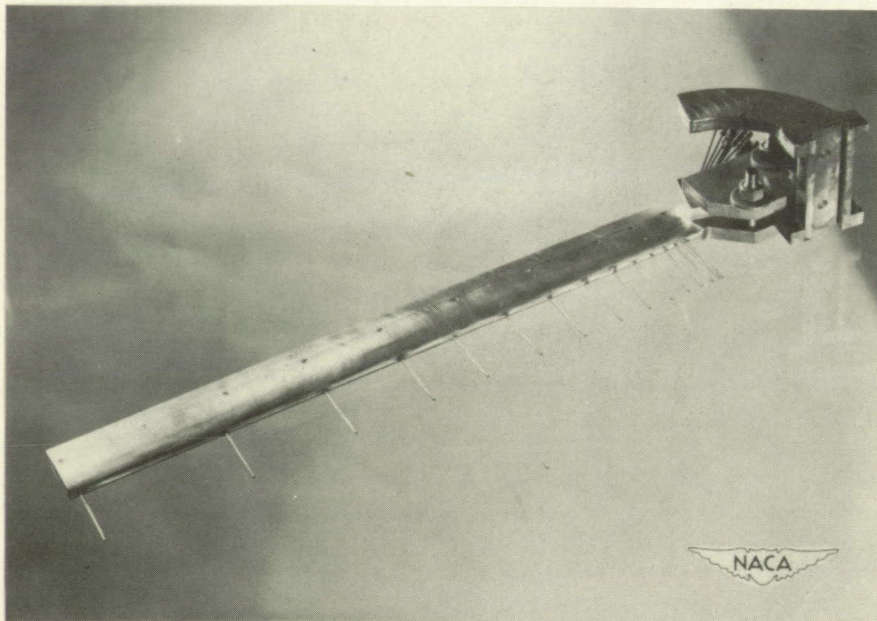


Figure 6.- Survey rake and carriage.



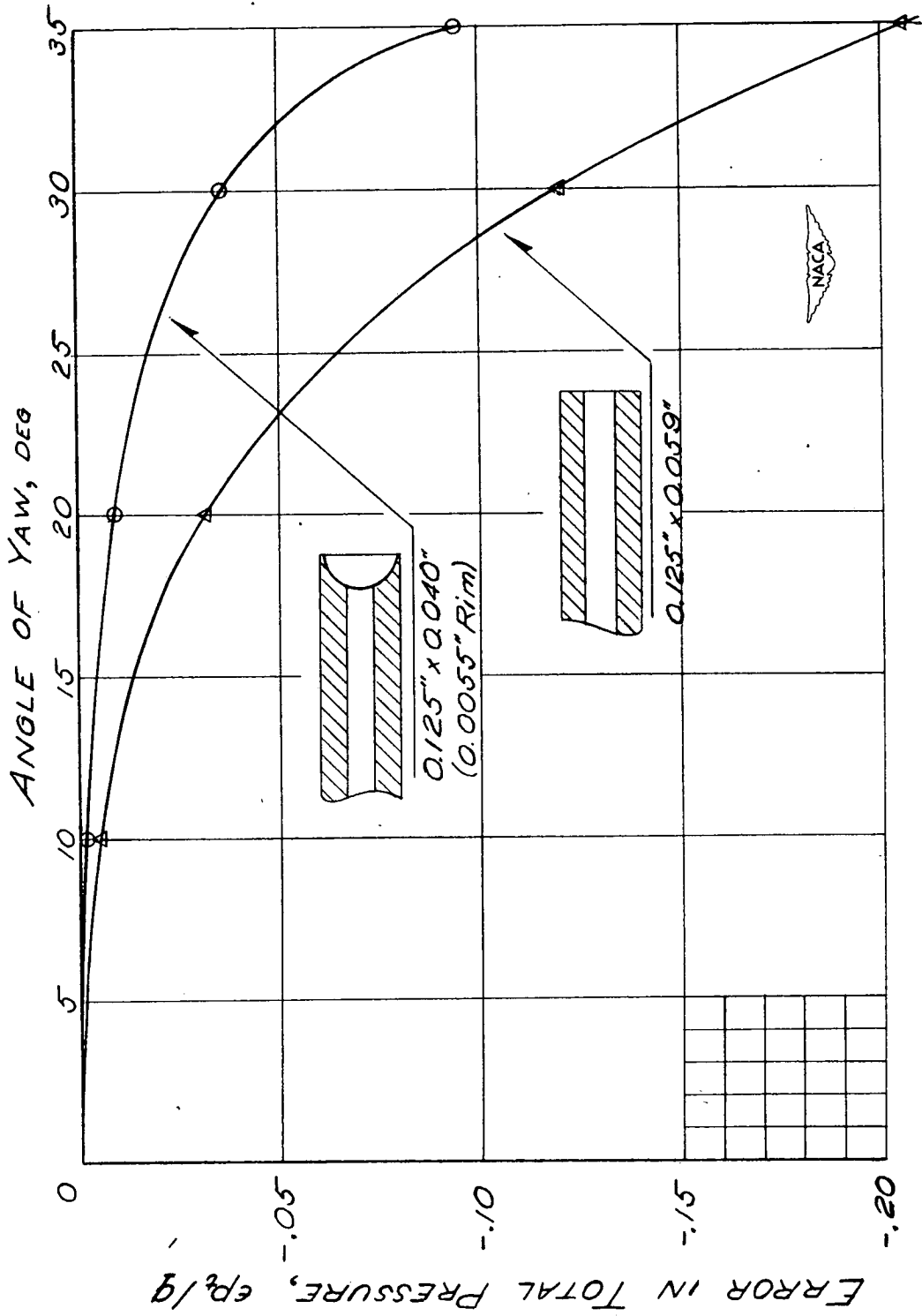


Figure 7.- Calibration curves for total-pressure tubes with flat and cupped tips.

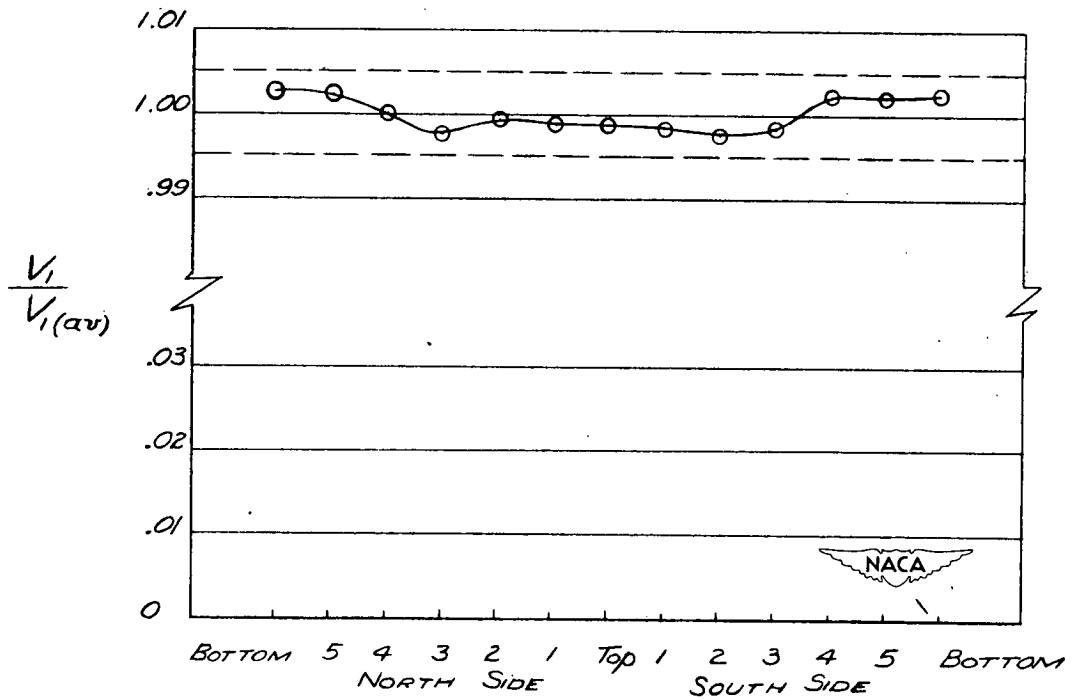
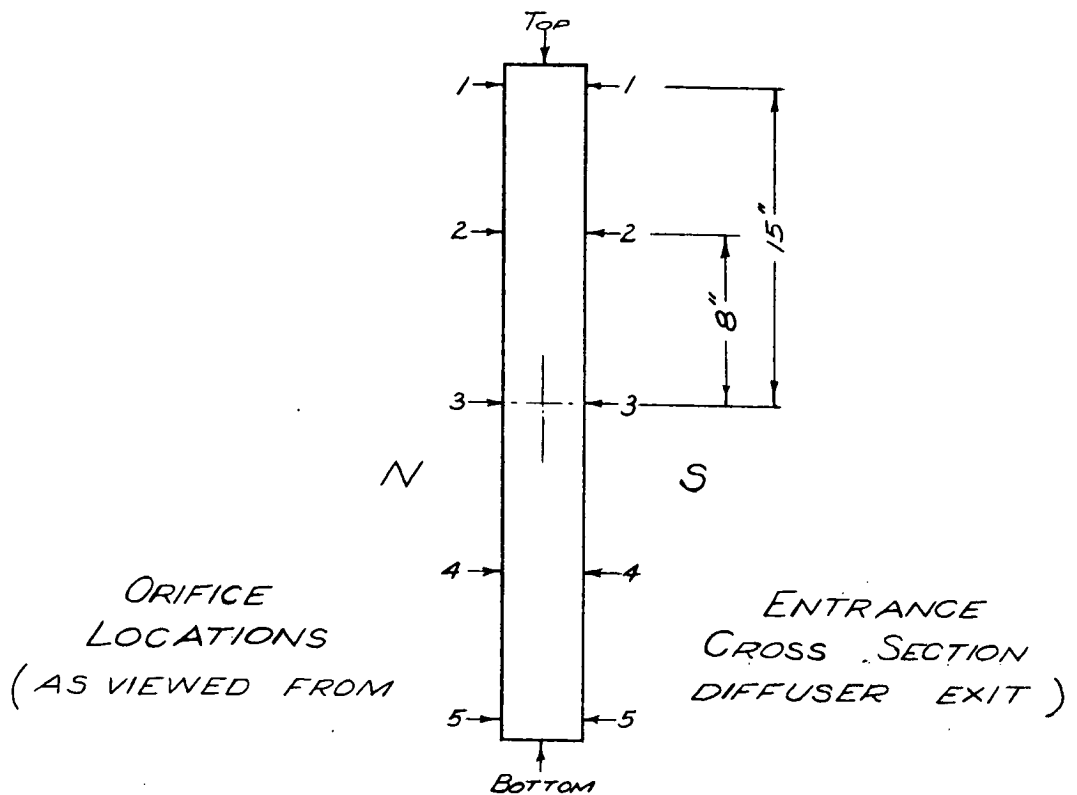
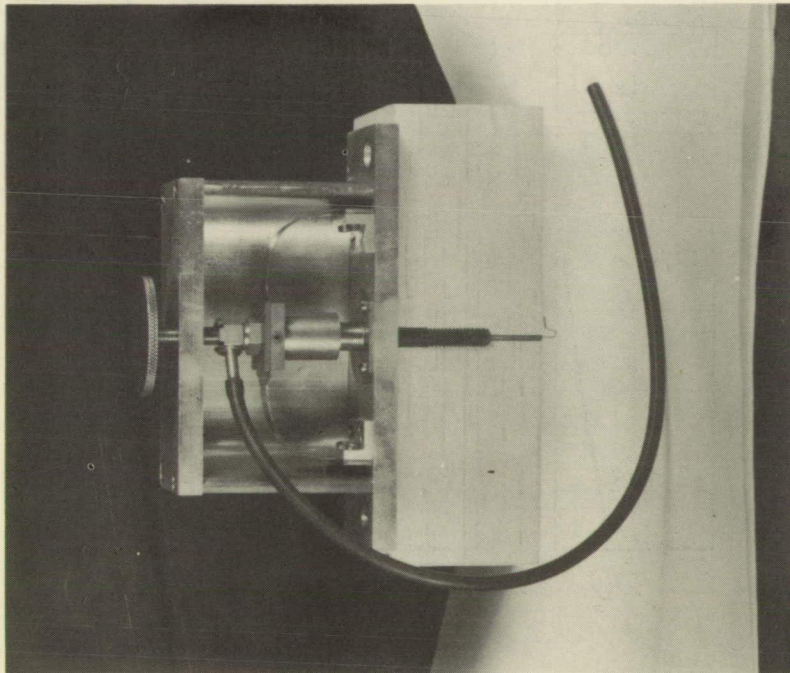
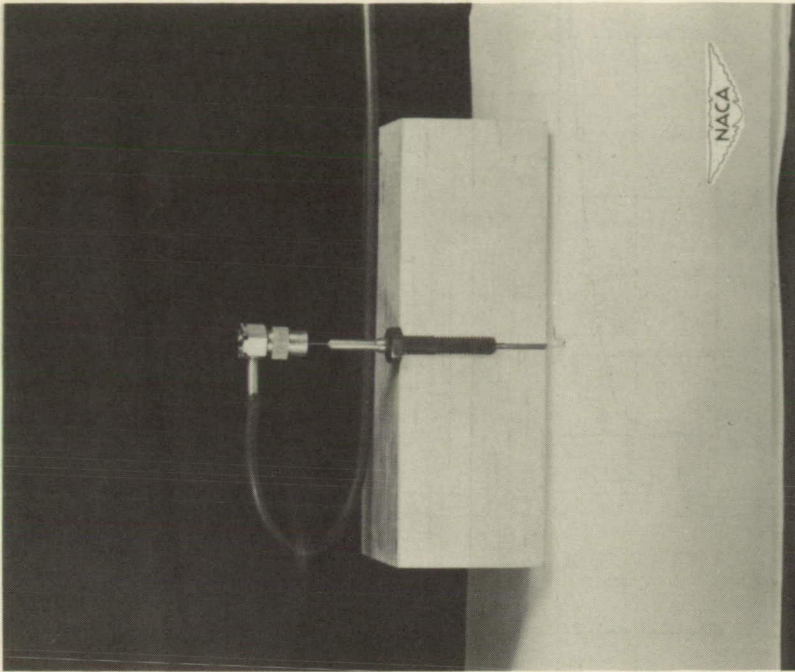


Figure 8.- Entrance velocity distribution.  $q_1 = 60$  pounds per square foot.



(a) Complete instrument installed on section of bellmouth wall.



(b) Pressure-transmitting elements positioned by micrometer screw.

Figure 9.- Boundary-layer survey instrument.

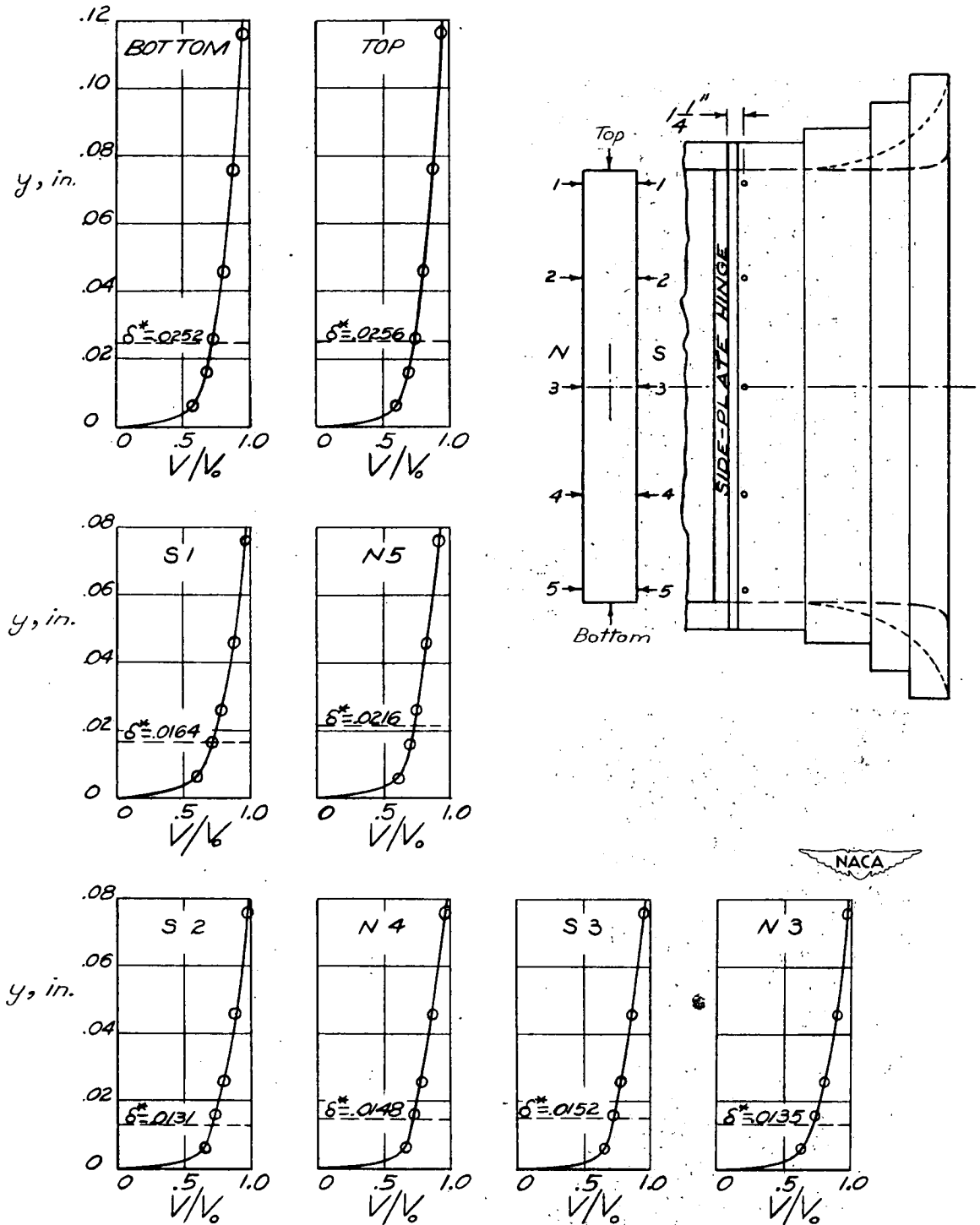


Figure 10.- Entrance boundary-layer profiles.



Figure 11.- Diffuser with central partition.

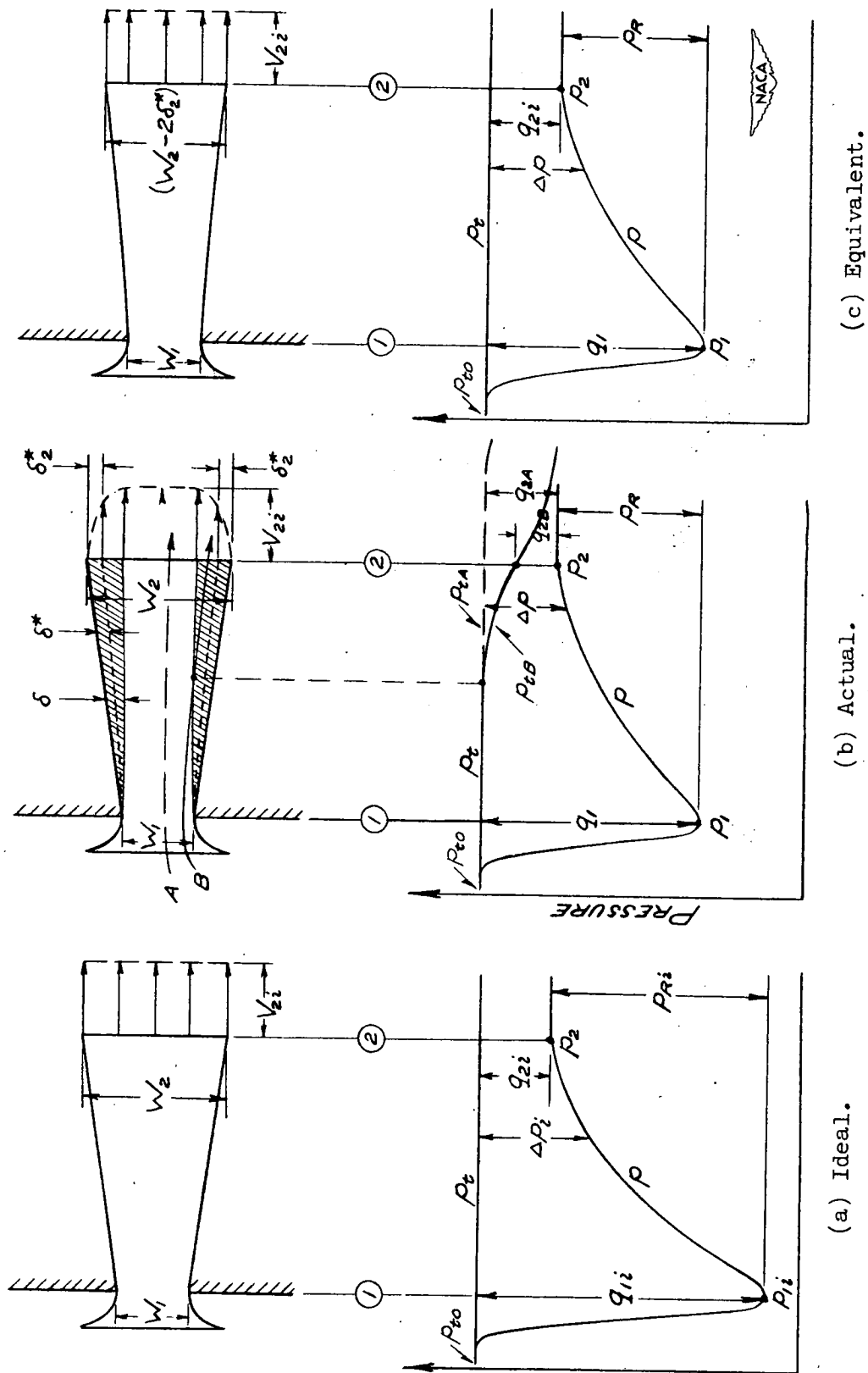


Figure 12.- Velocities and pressures in ideal, actual, and equivalent diffusers.



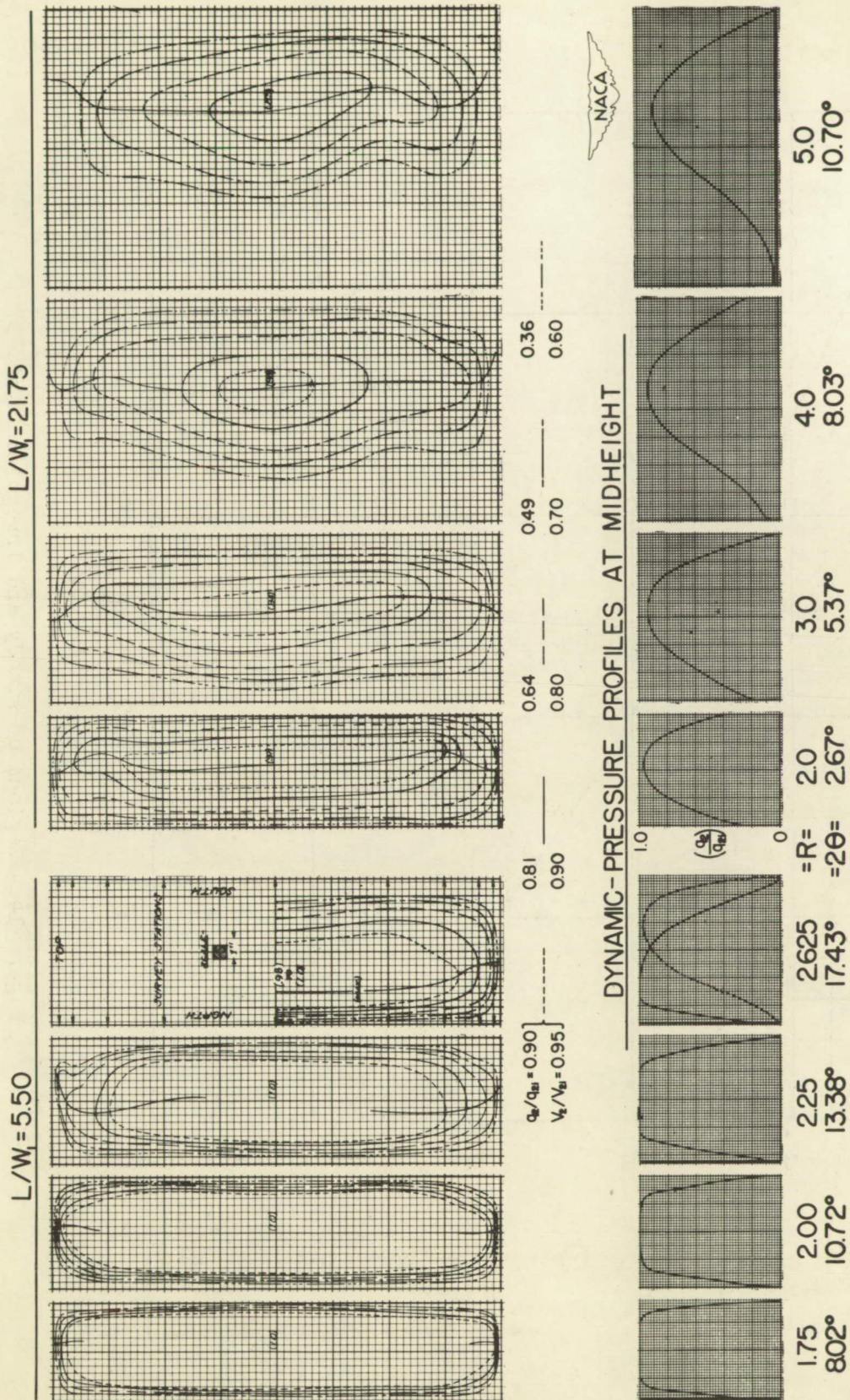


Figure 13.- Typical distributions of dynamic pressure at exit.

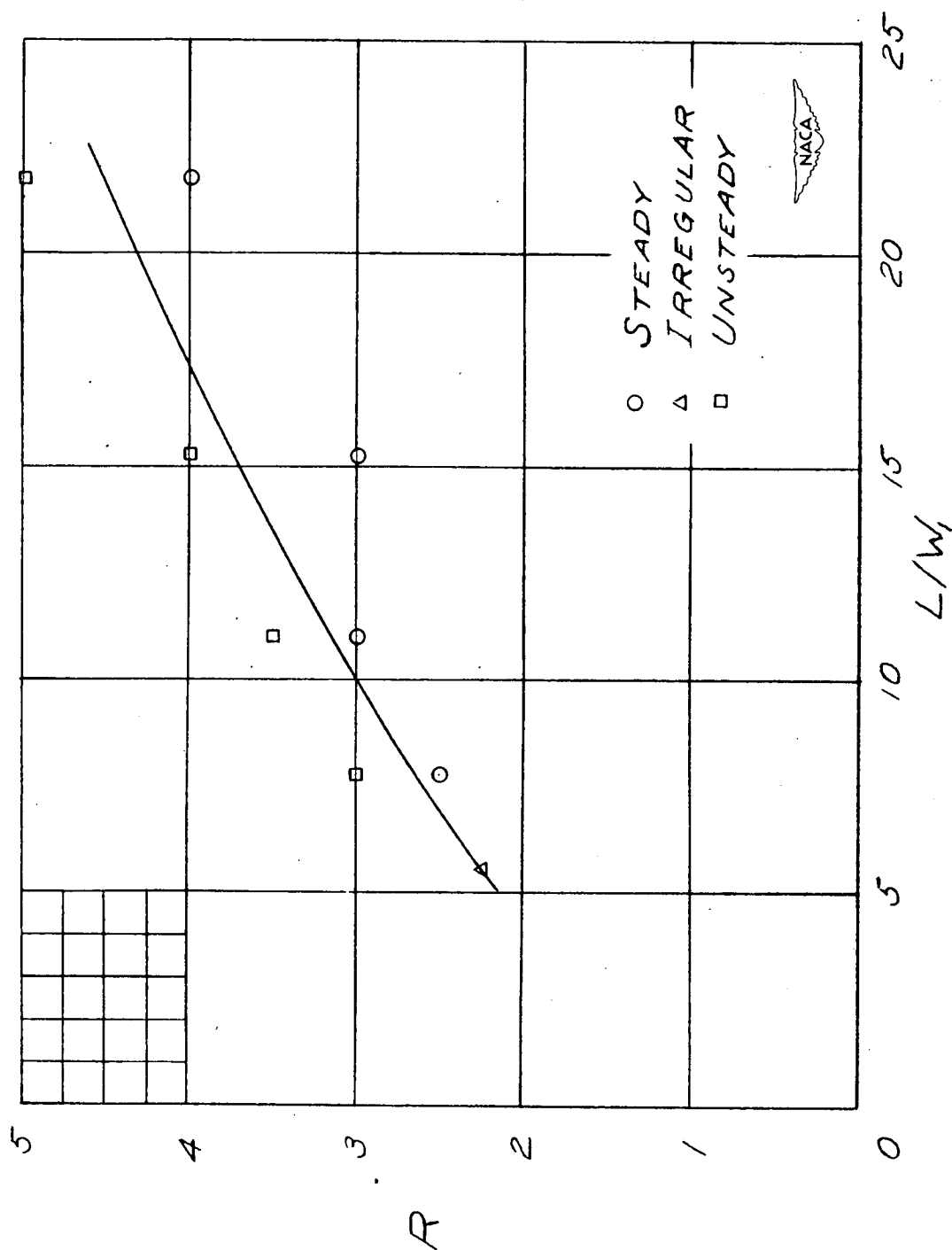


Figure 14.- Regions of steady and irregular flow.



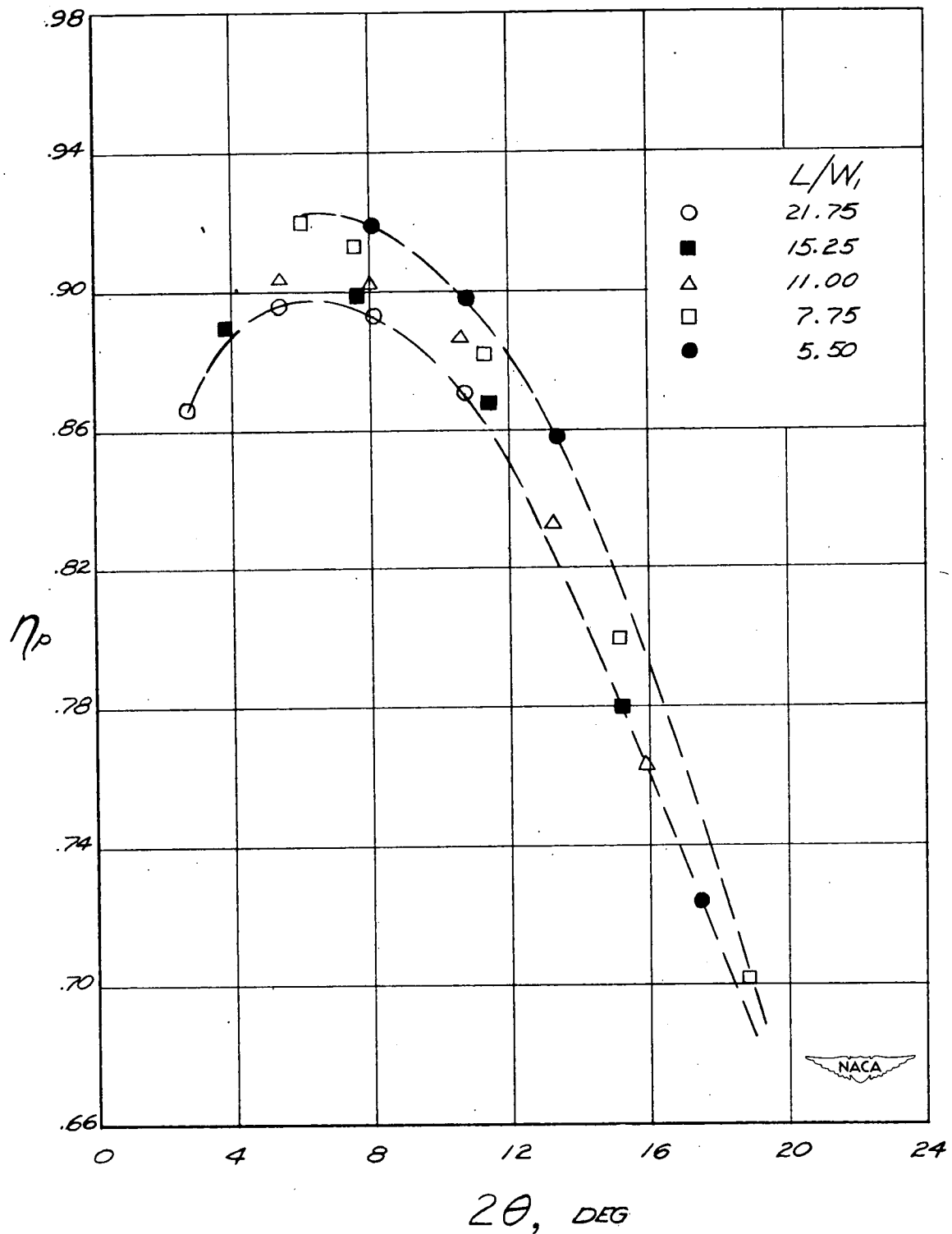


Figure 15.- Variation of pressure efficiency with divergence angle.

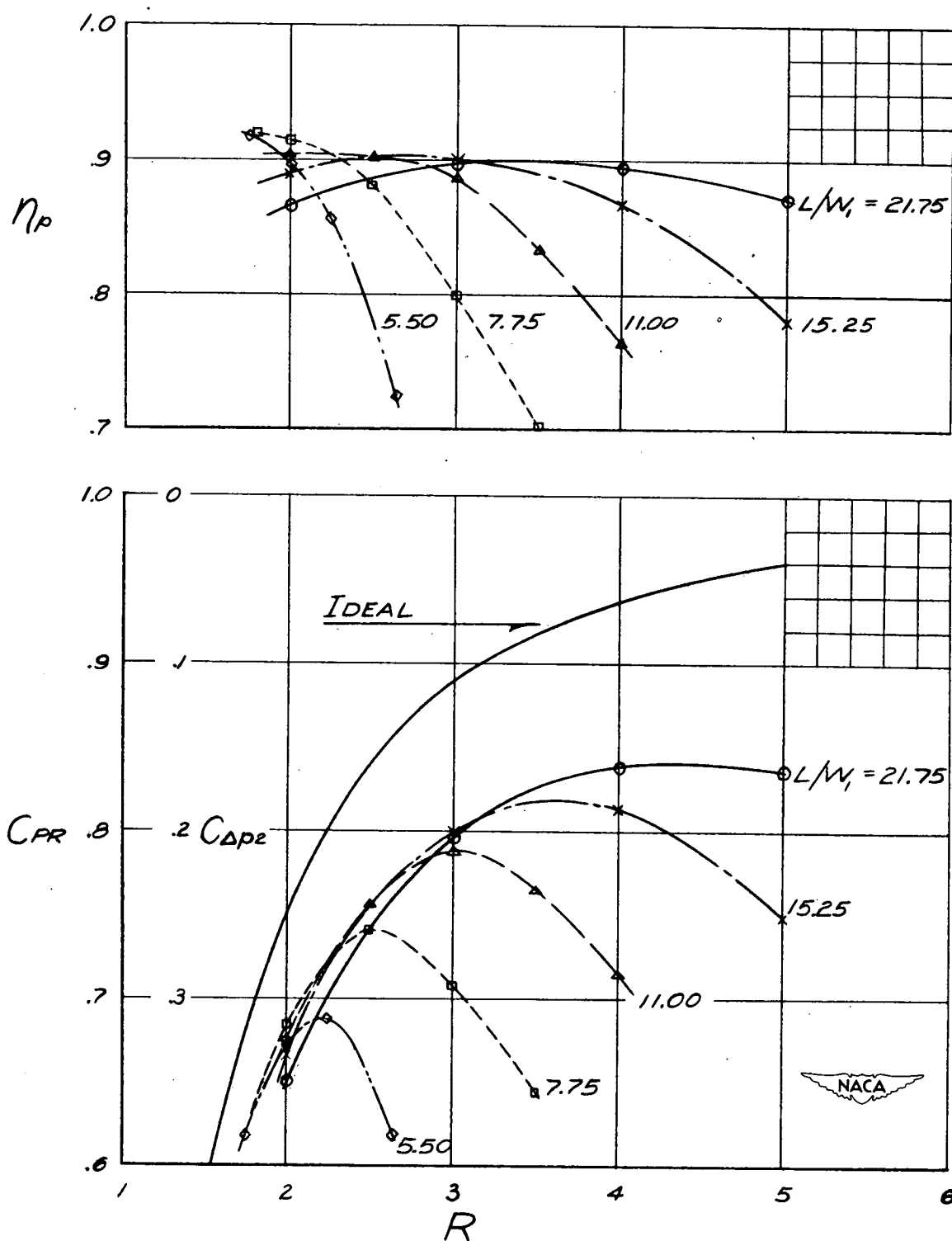


Figure 16.- Variations of pressure efficiency and pressure-recovery coefficient with area ratio.

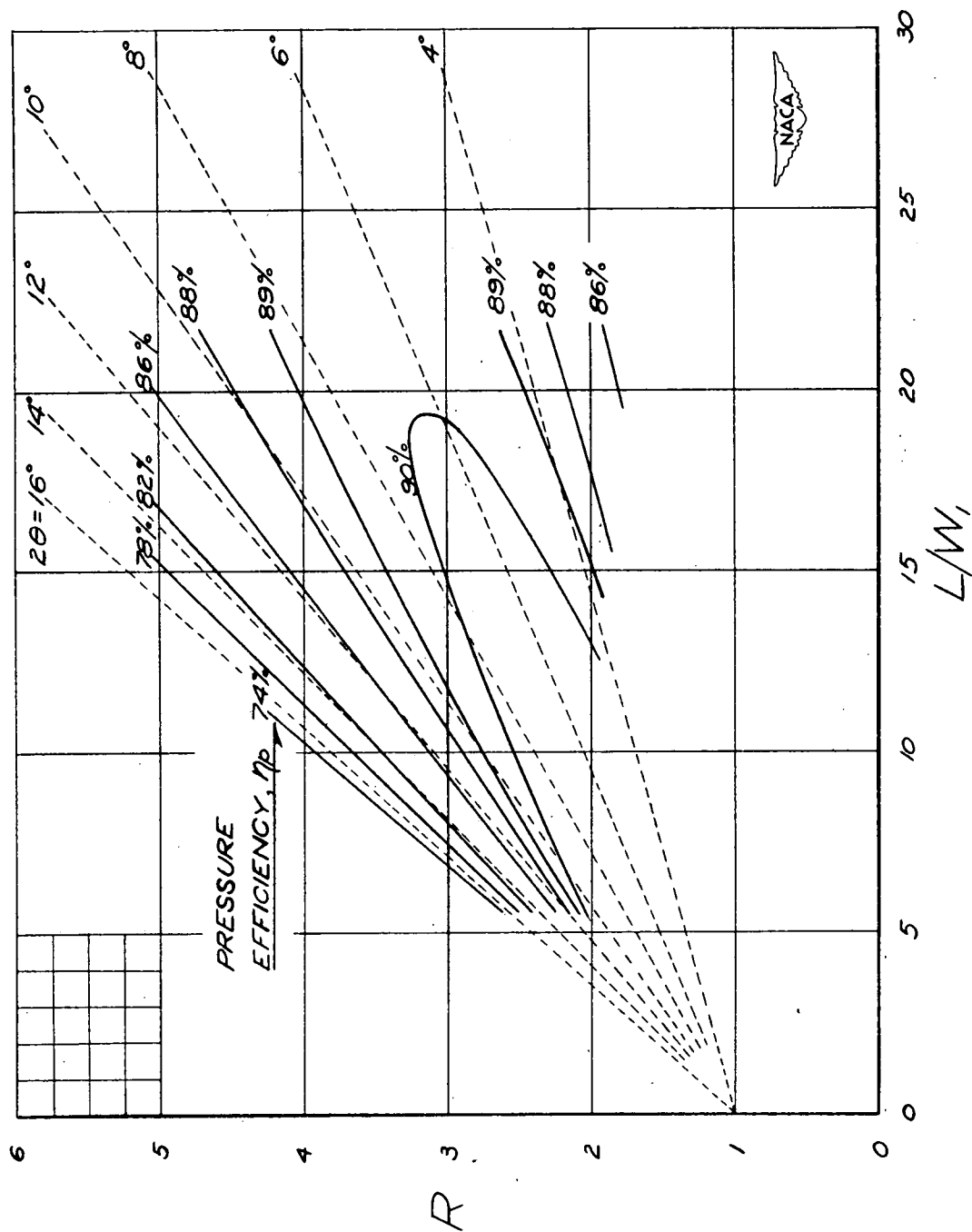


Figure 17.- Contours of constant pressure efficiency.

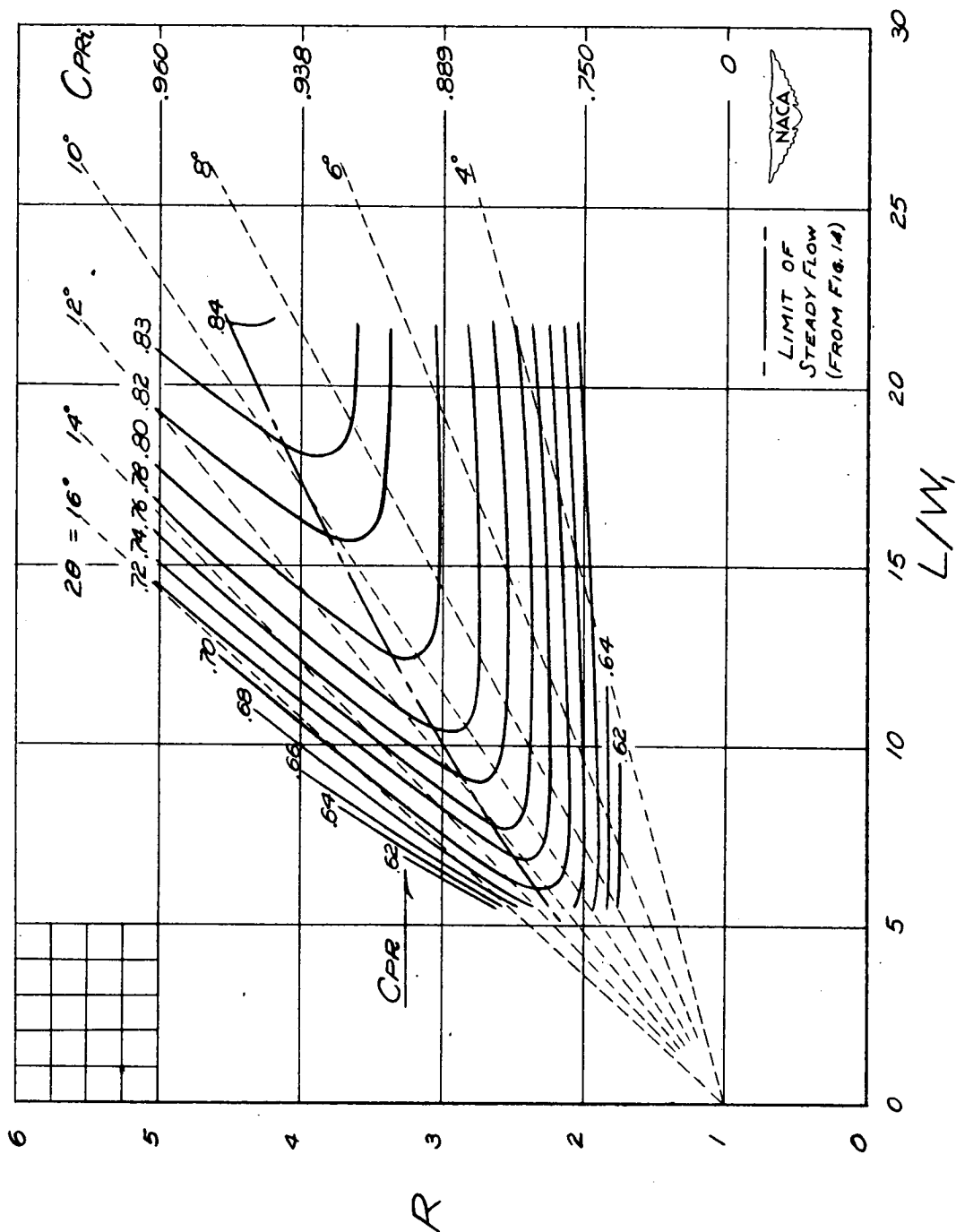


Figure 18.- Contours of constant pressure-recovery coefficient.

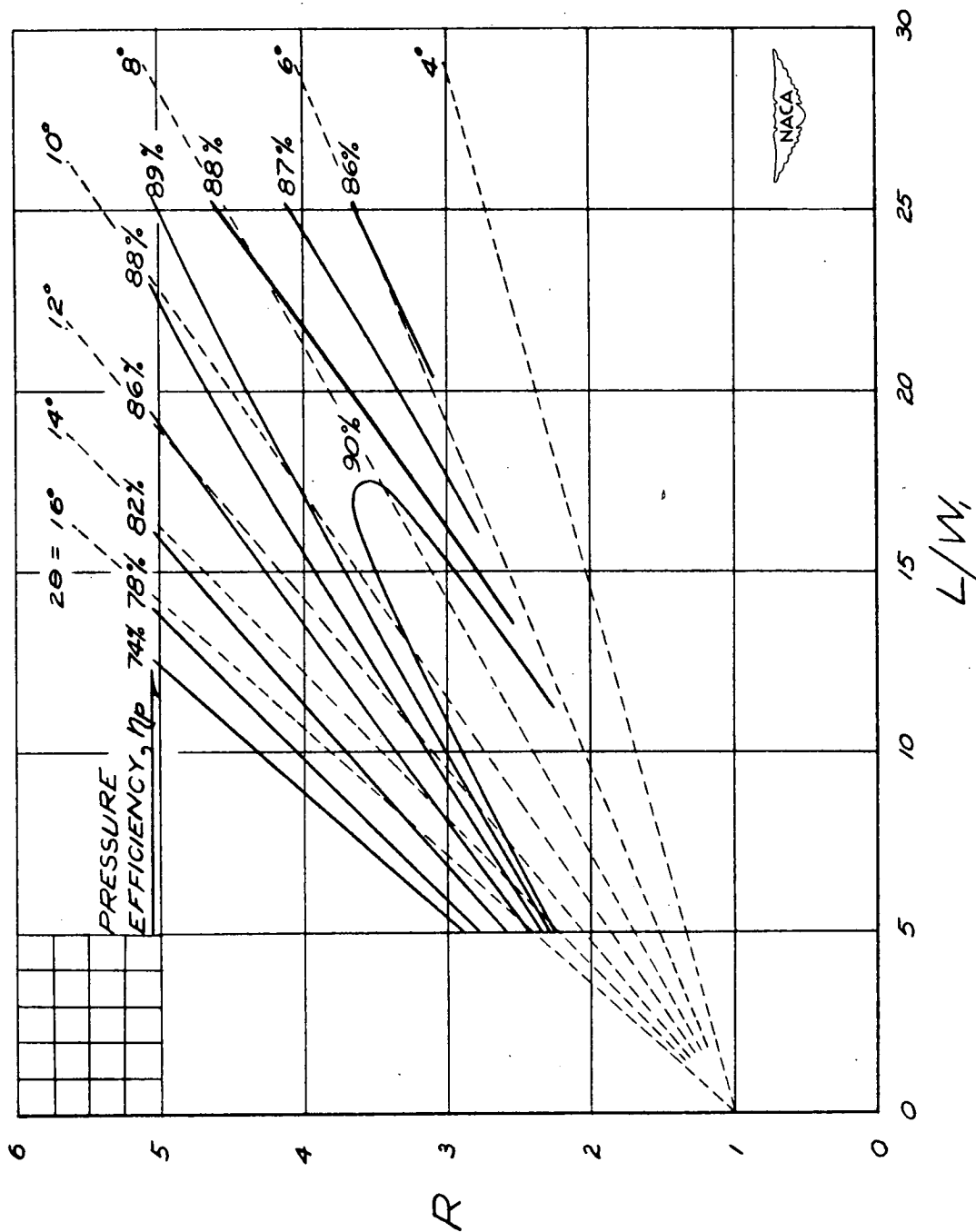


Figure 19.- Contours of constant pressure efficiency (Gibson's results, reference 2).

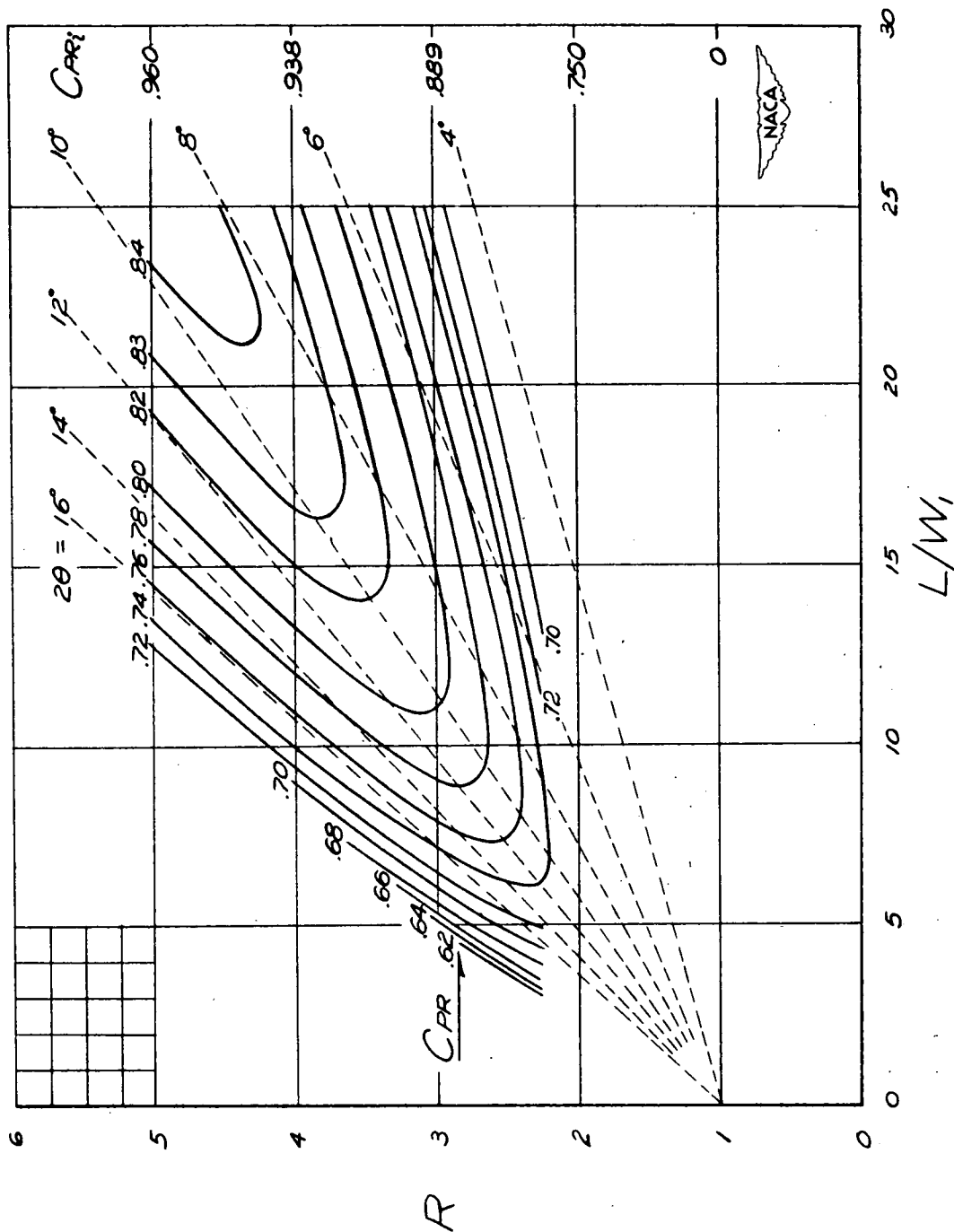
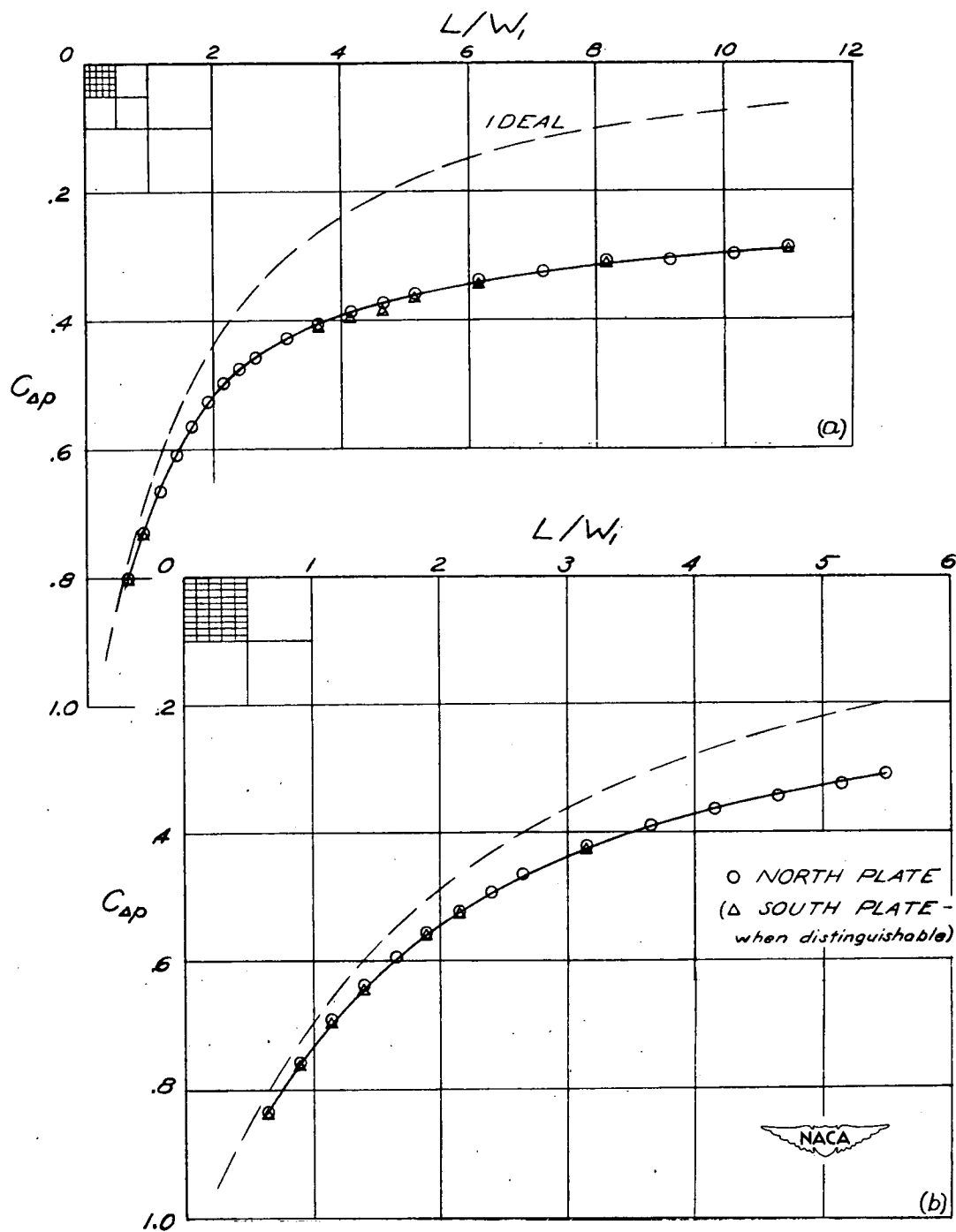


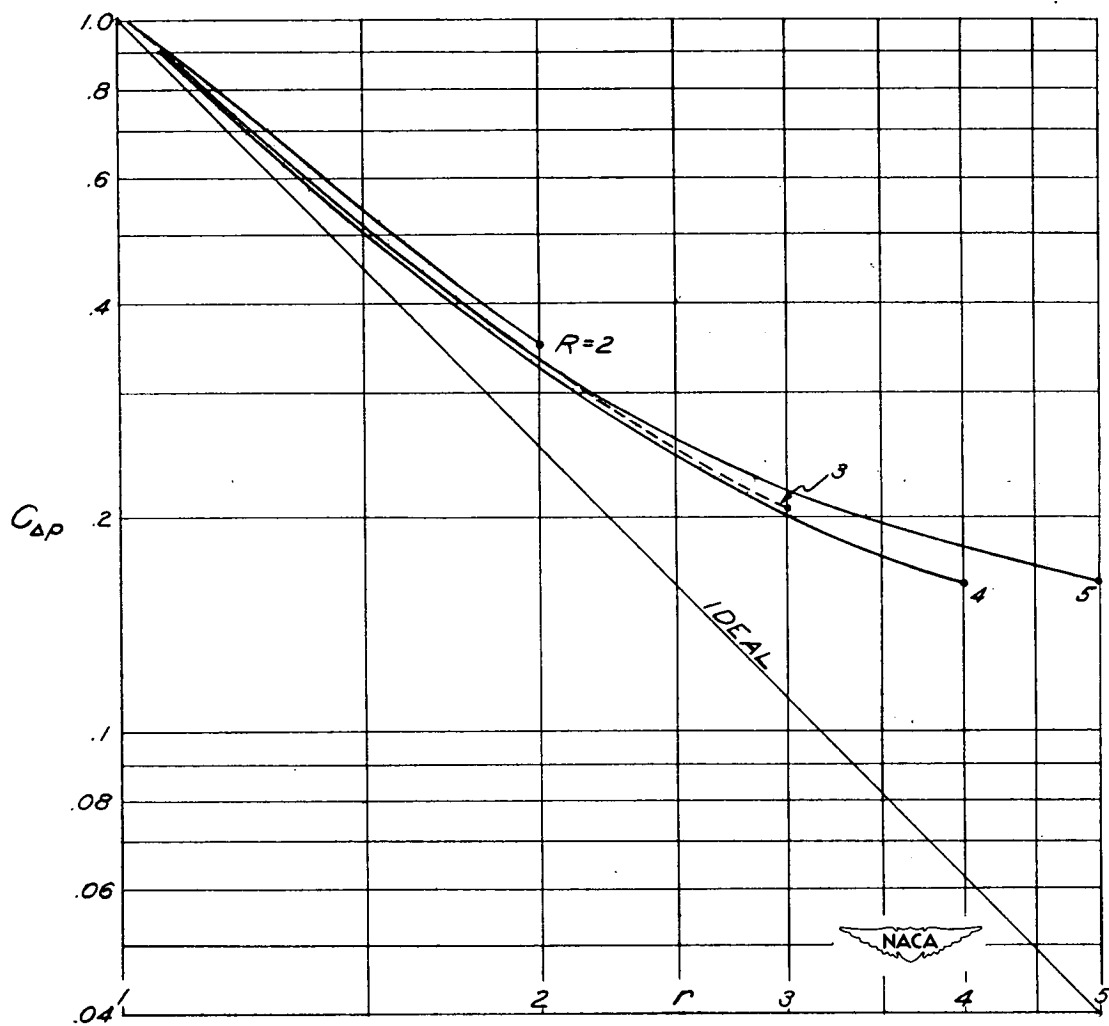
Figure 20.- Contours of constant pressure-recovery coefficient (Gibson's results, reference 2).



(a)  $L/W_1 = 11.00$ ;  $R = 4.00$ .

(b)  $L/W_1 = 5.50$ ;  $R = 2.25$ .

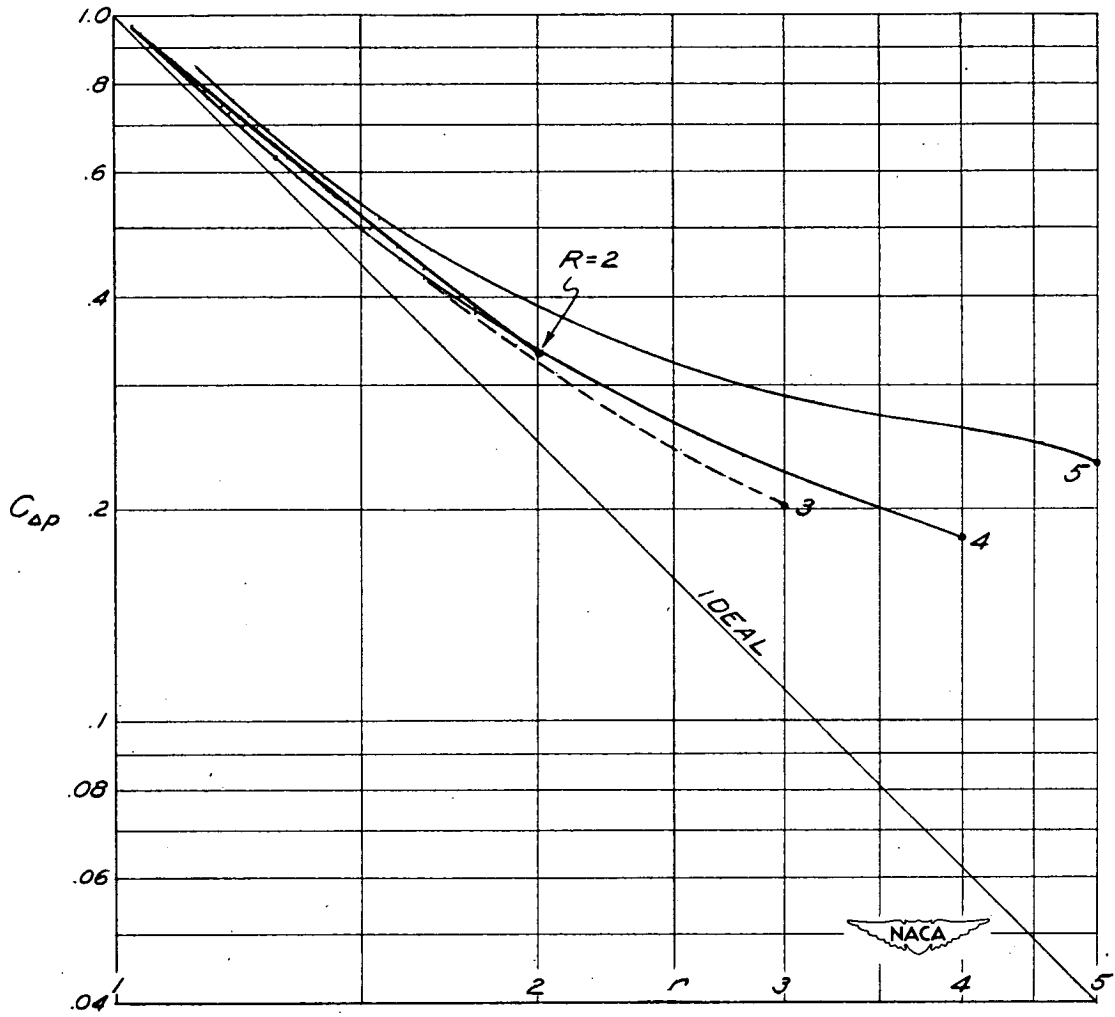
Figure 21.- Distributions of pressure along divergent walls.



(a)  $L/W_1 = 21.75$ .

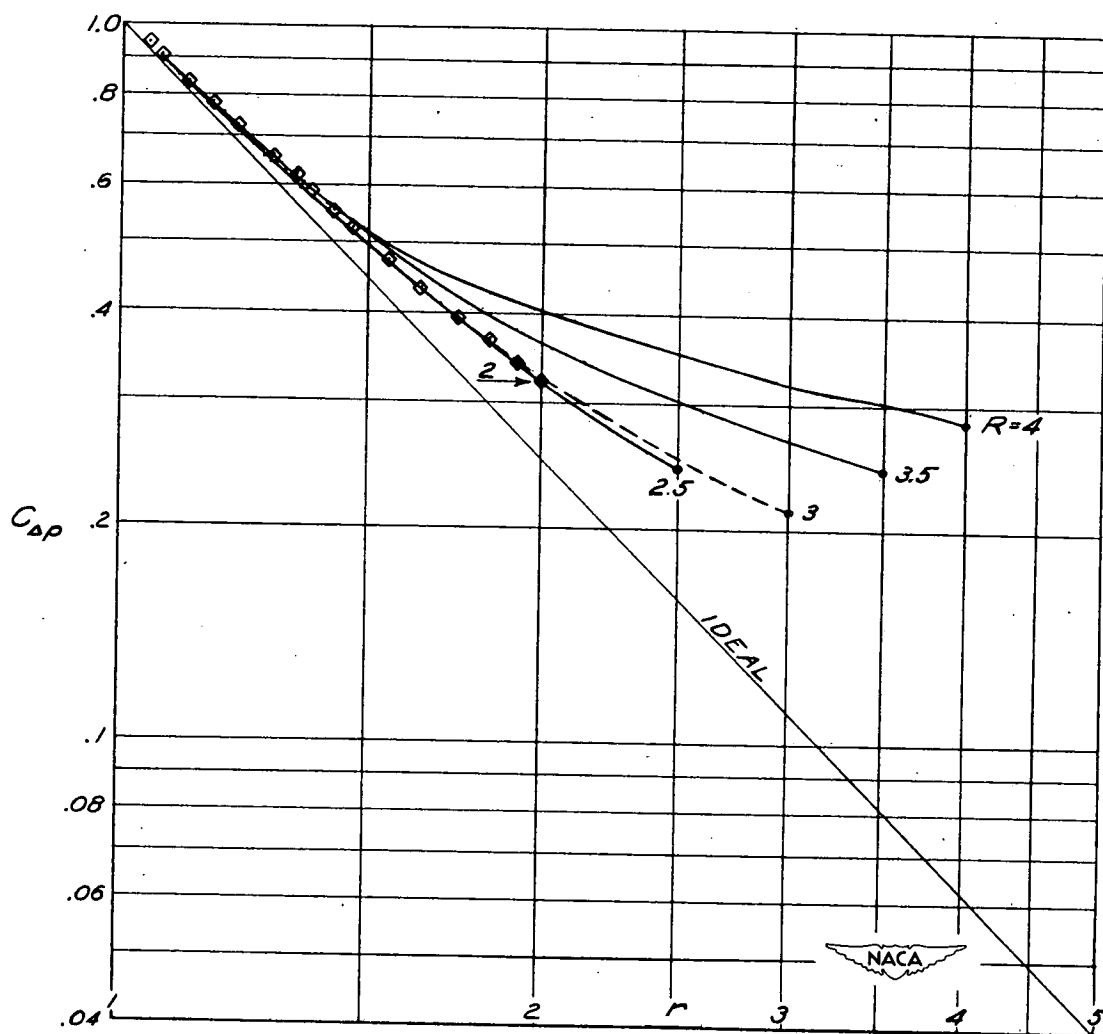
Figure 22.- Variation of static pressure with local area ratio.





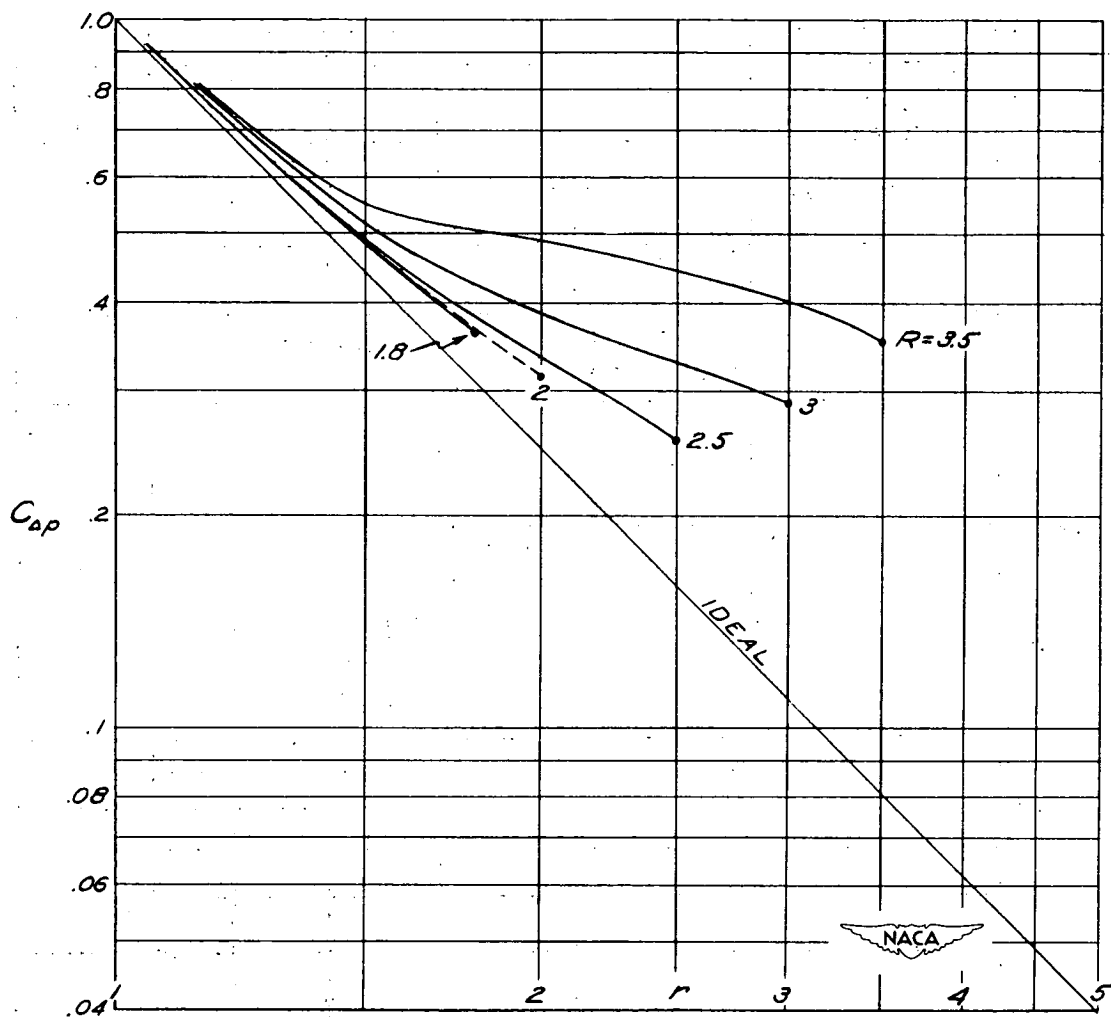
(b)  $L/W_1 = 15.25$ .

Figure 22.- Continued.



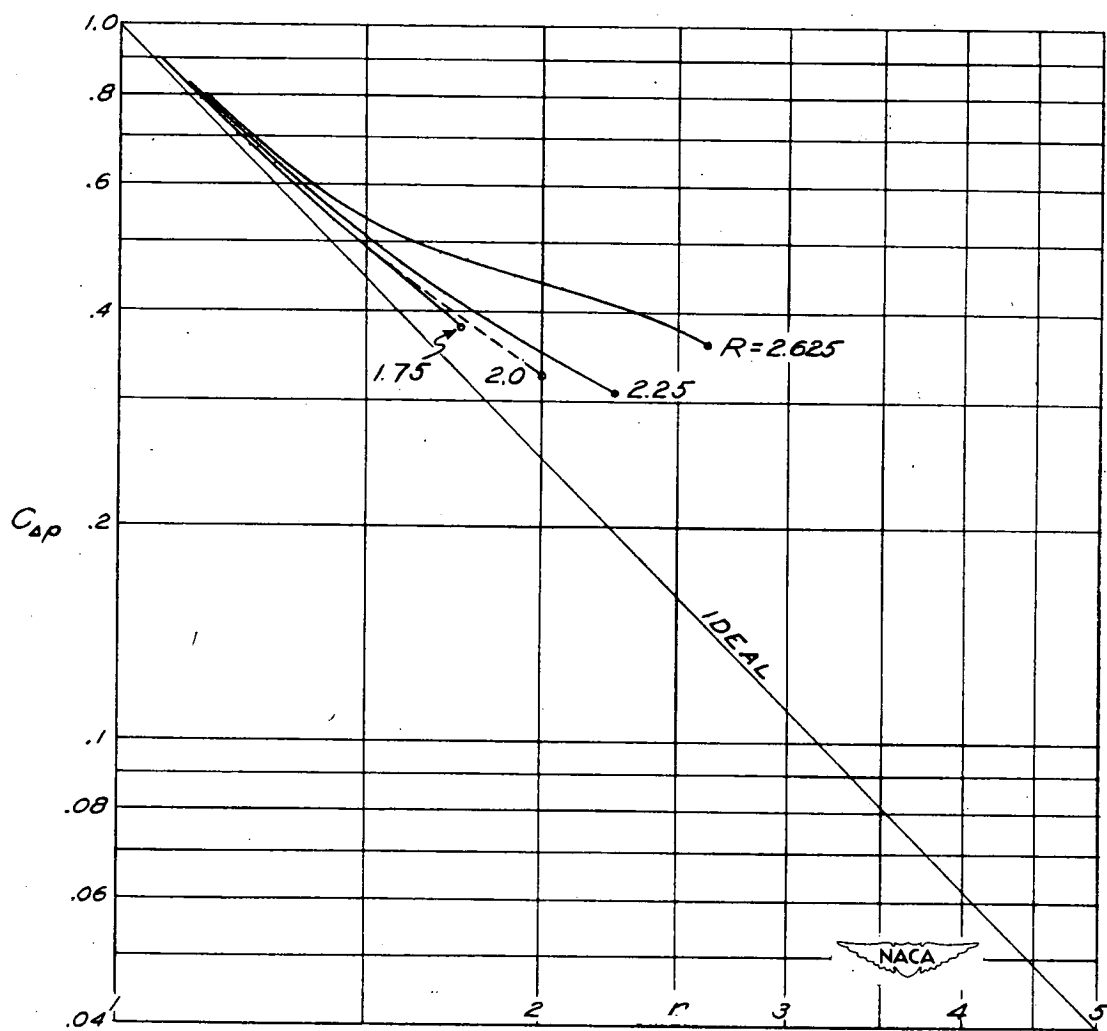
(c)  $L/W_1 = 11.00$ .

Figure 22.- Continued.



(d)  $L/W_1 = 7.75$ .

Figure 22.- Continued.



(e)  $L/W_1 = 5.50$ .

Figure 22.- Concluded.

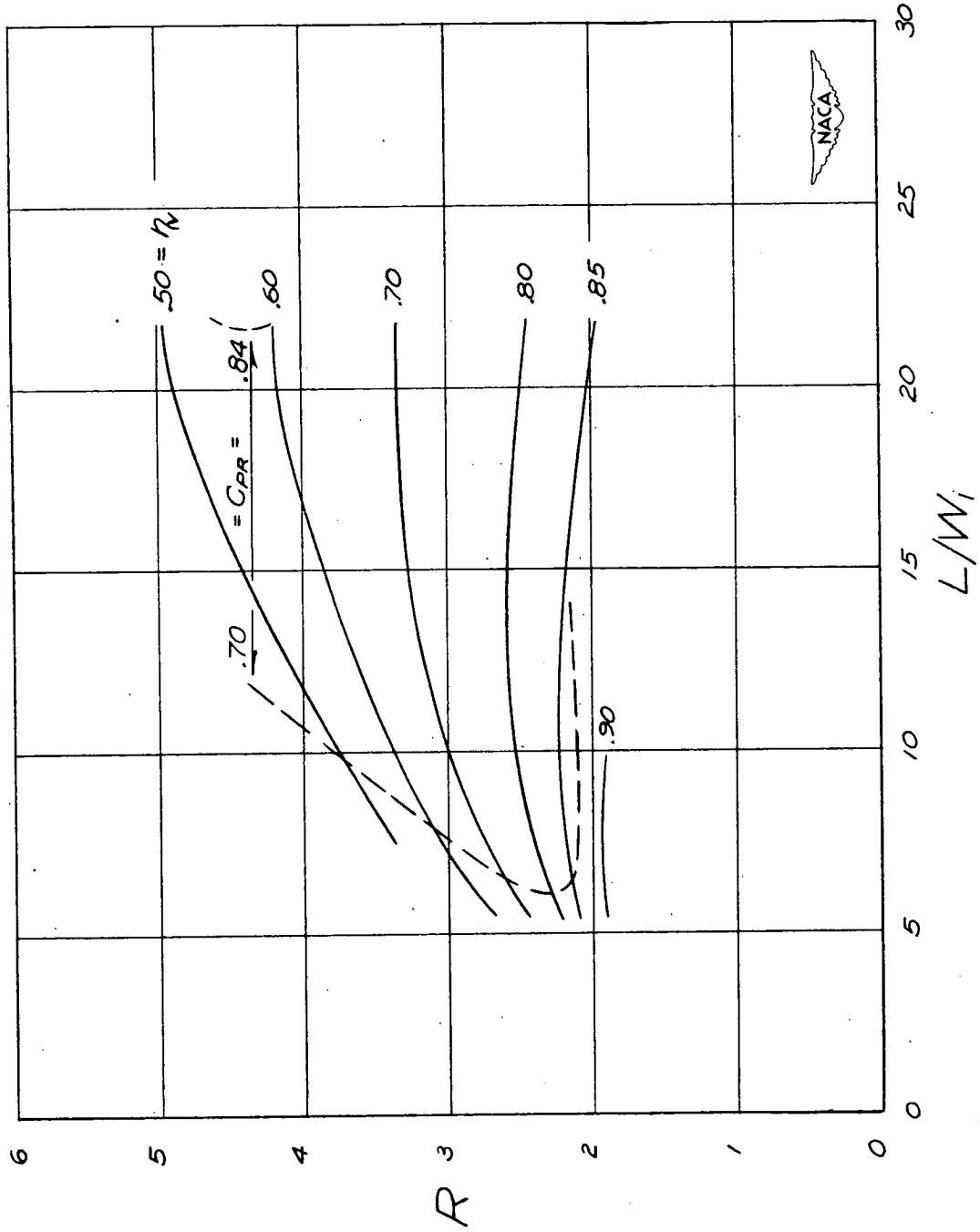


Figure 23.- Contours of constant volumetric efficiency.

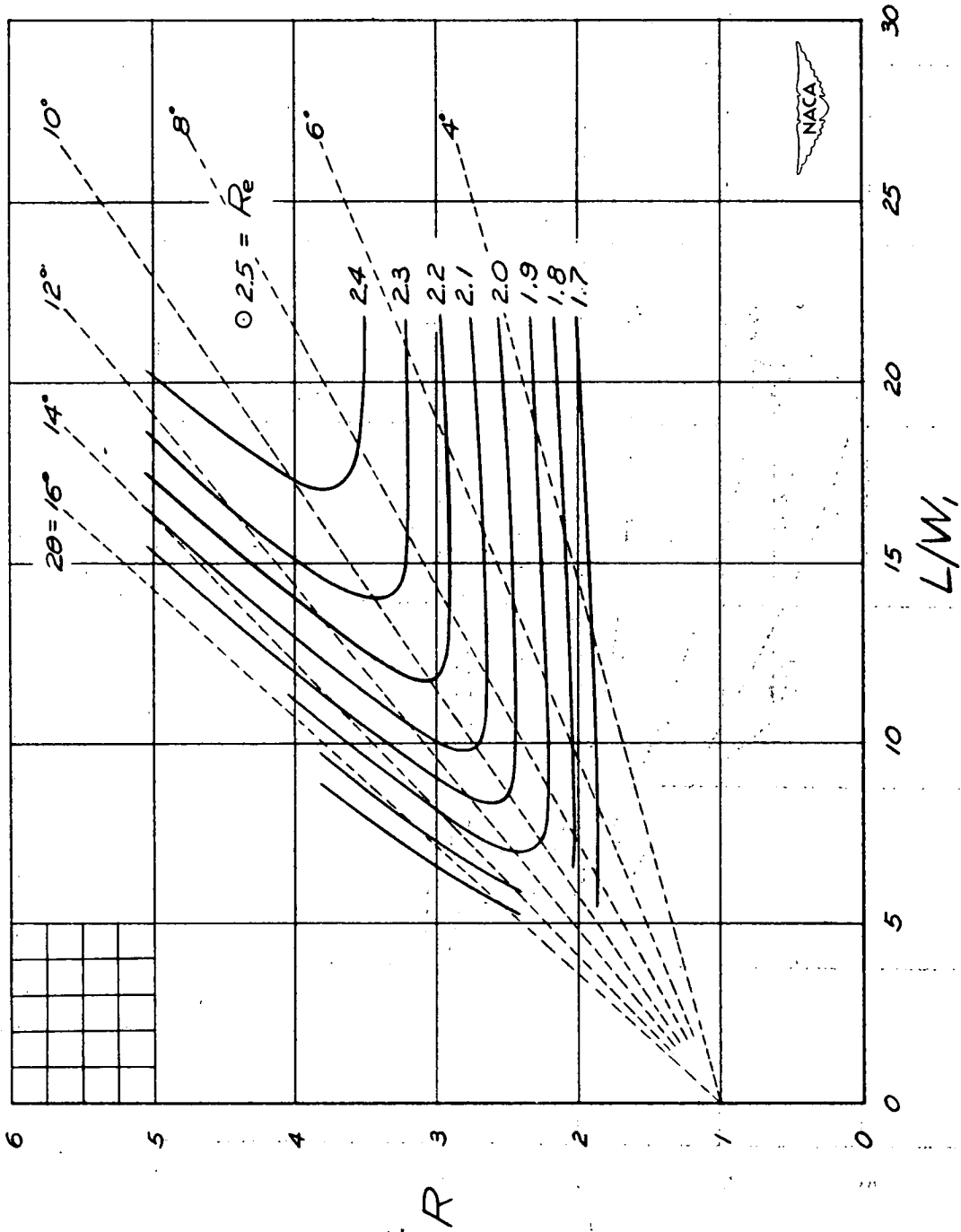


Figure 24.- Contours of constant effective area ratio.

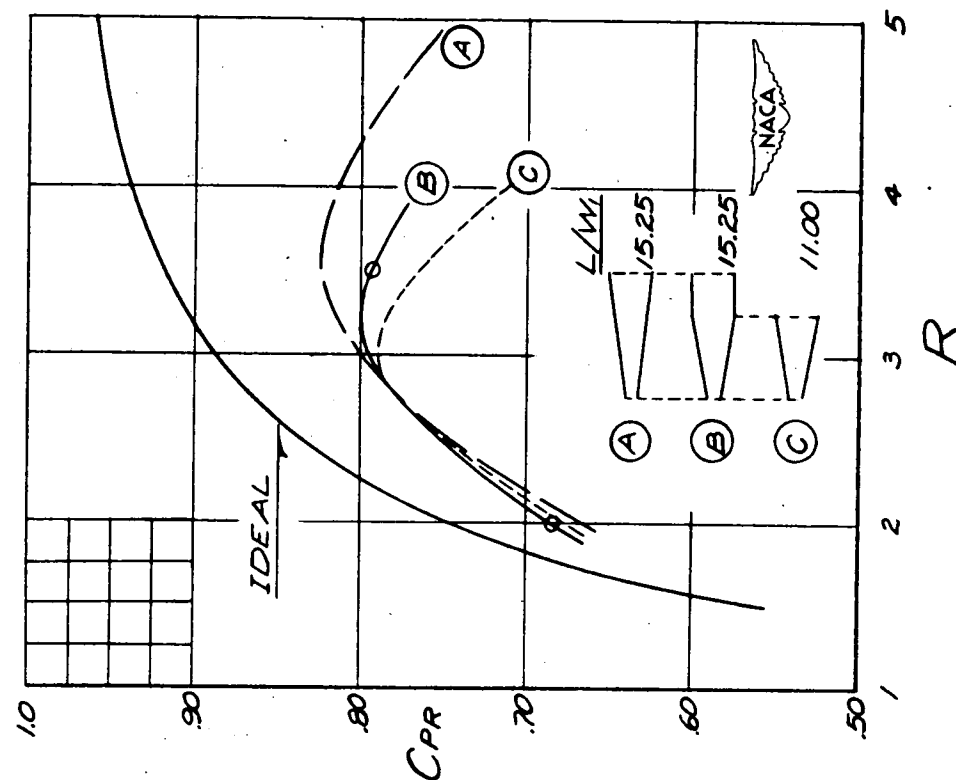


Figure 25.- Effects of asymmetry on pressure recovery.

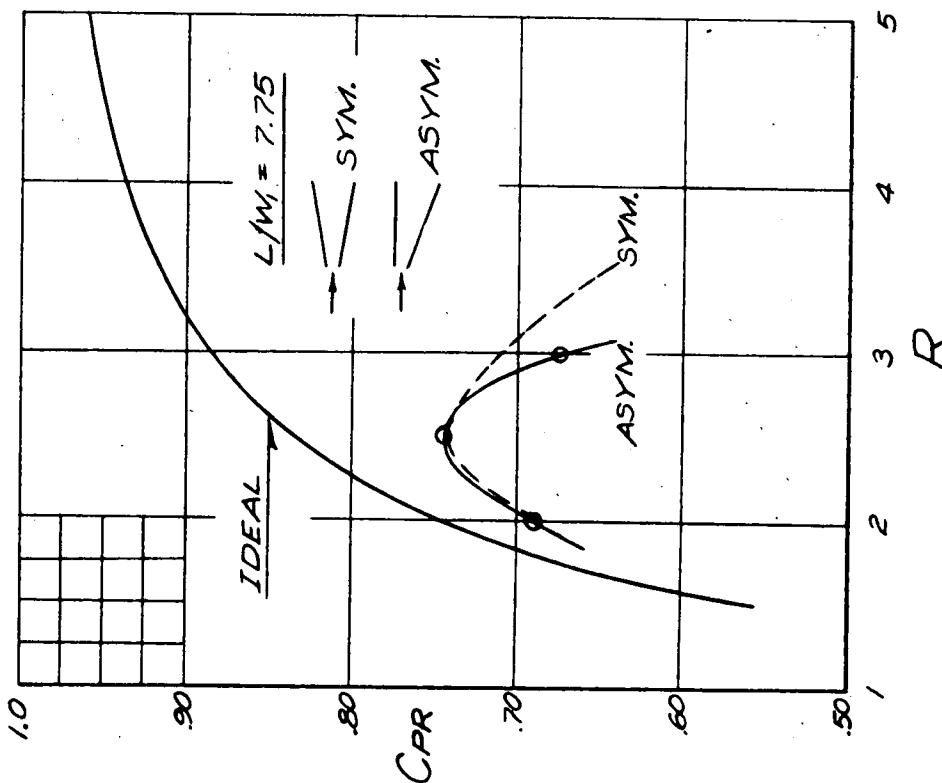


Figure 26.- Effects of adding constant-section exit duct.

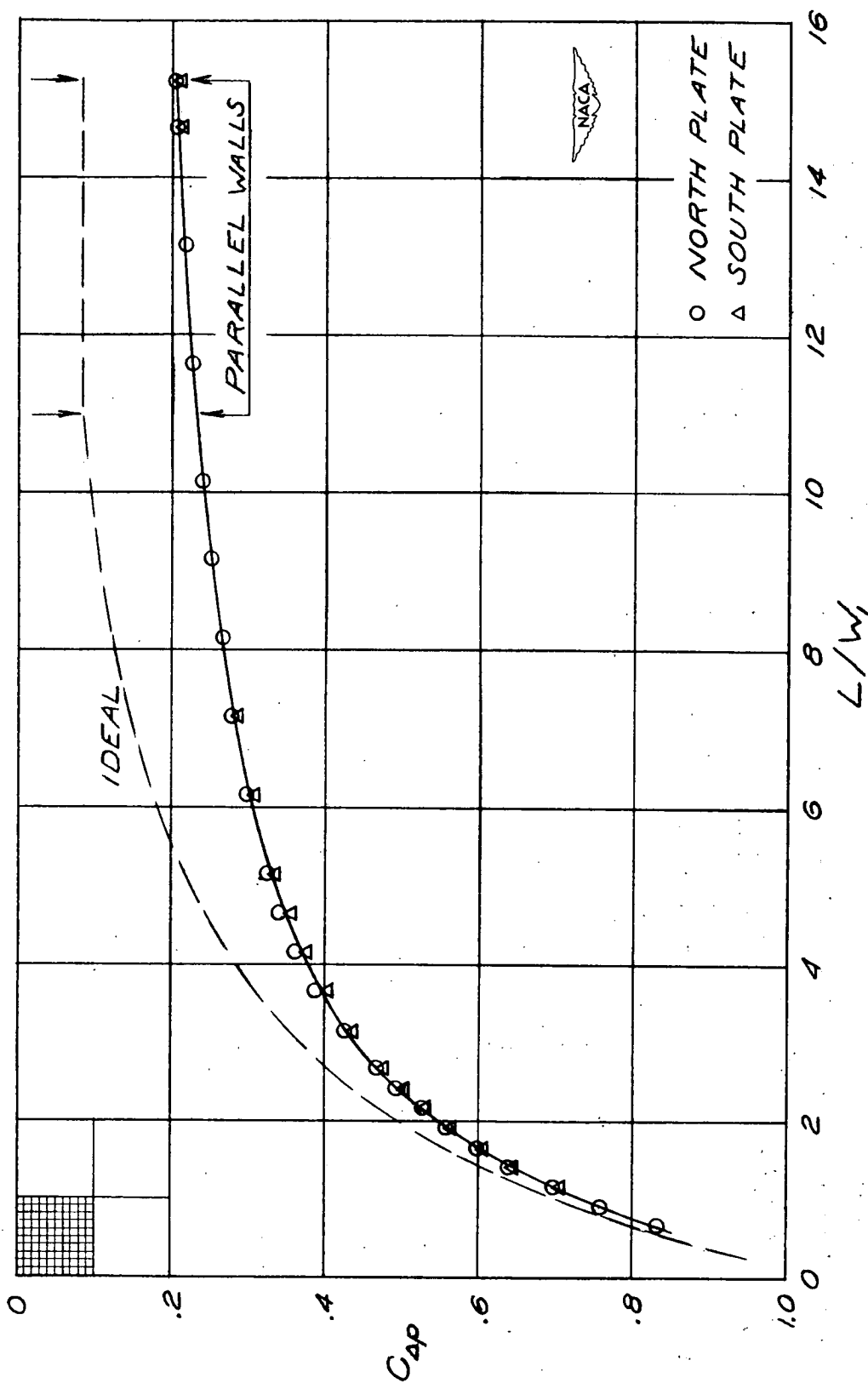


Figure 27.- Divergent-wall pressure distribution in extended diffuser.  
 $L/W_1 = 15.25$ ;  $R = 3.50$ .



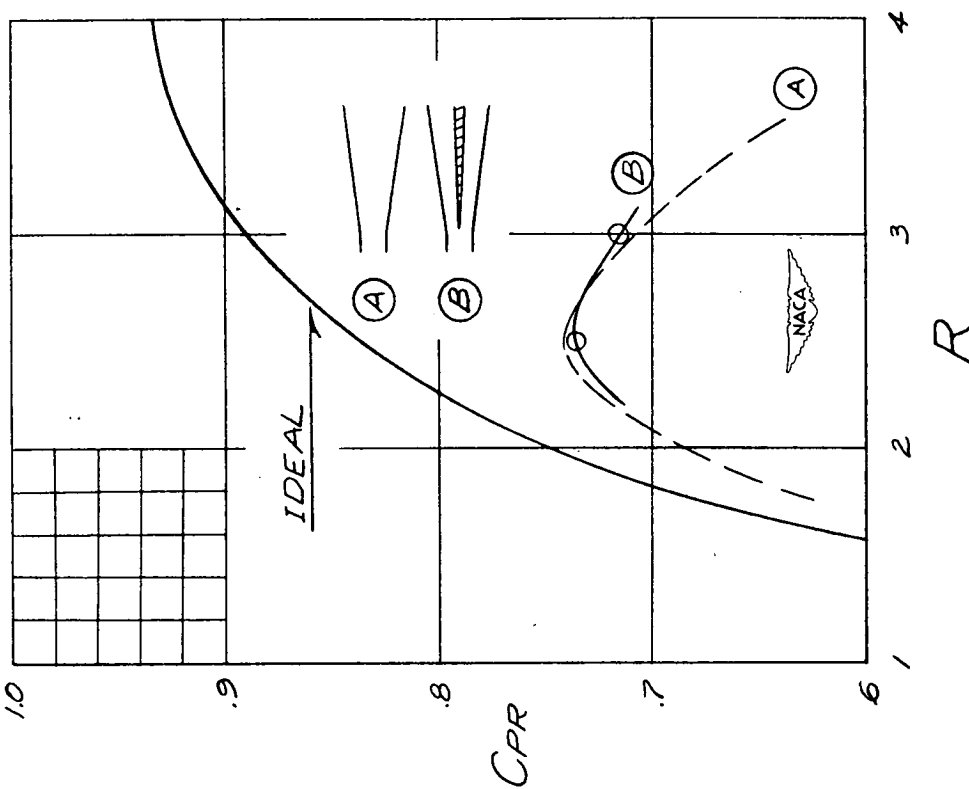


Figure 29.- Effects of central wedge on pressure recovery.  
 $L/W_1 = 7.75$ .

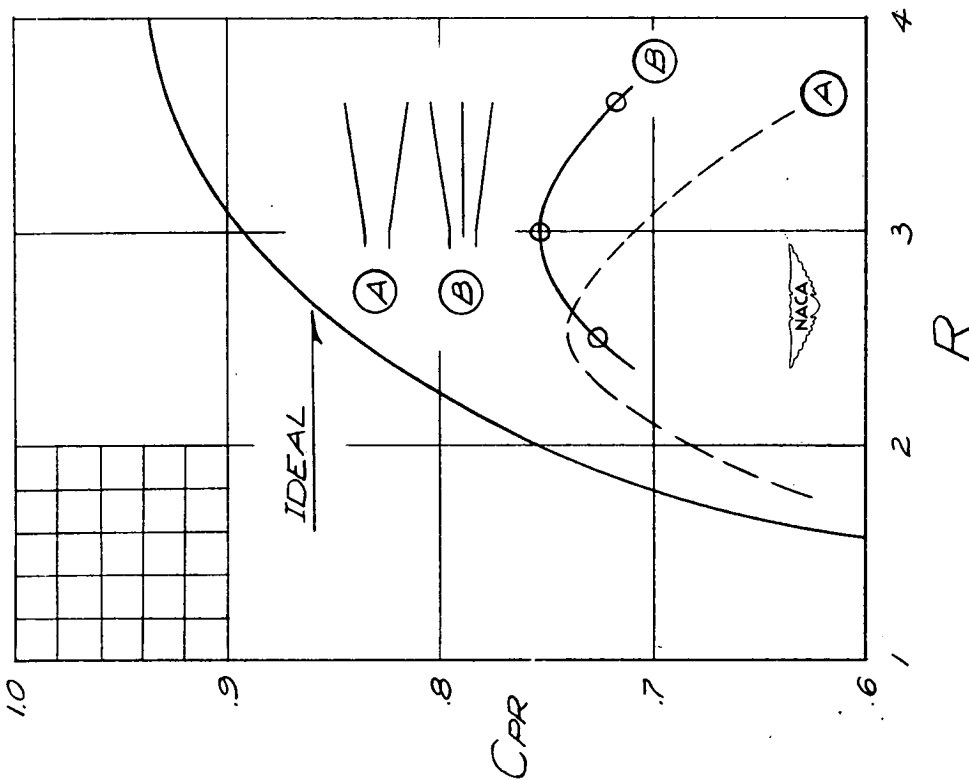


Figure 28.- Effects of central partition on pressure recovery.  
 $L/W_1 = 7.75$ .

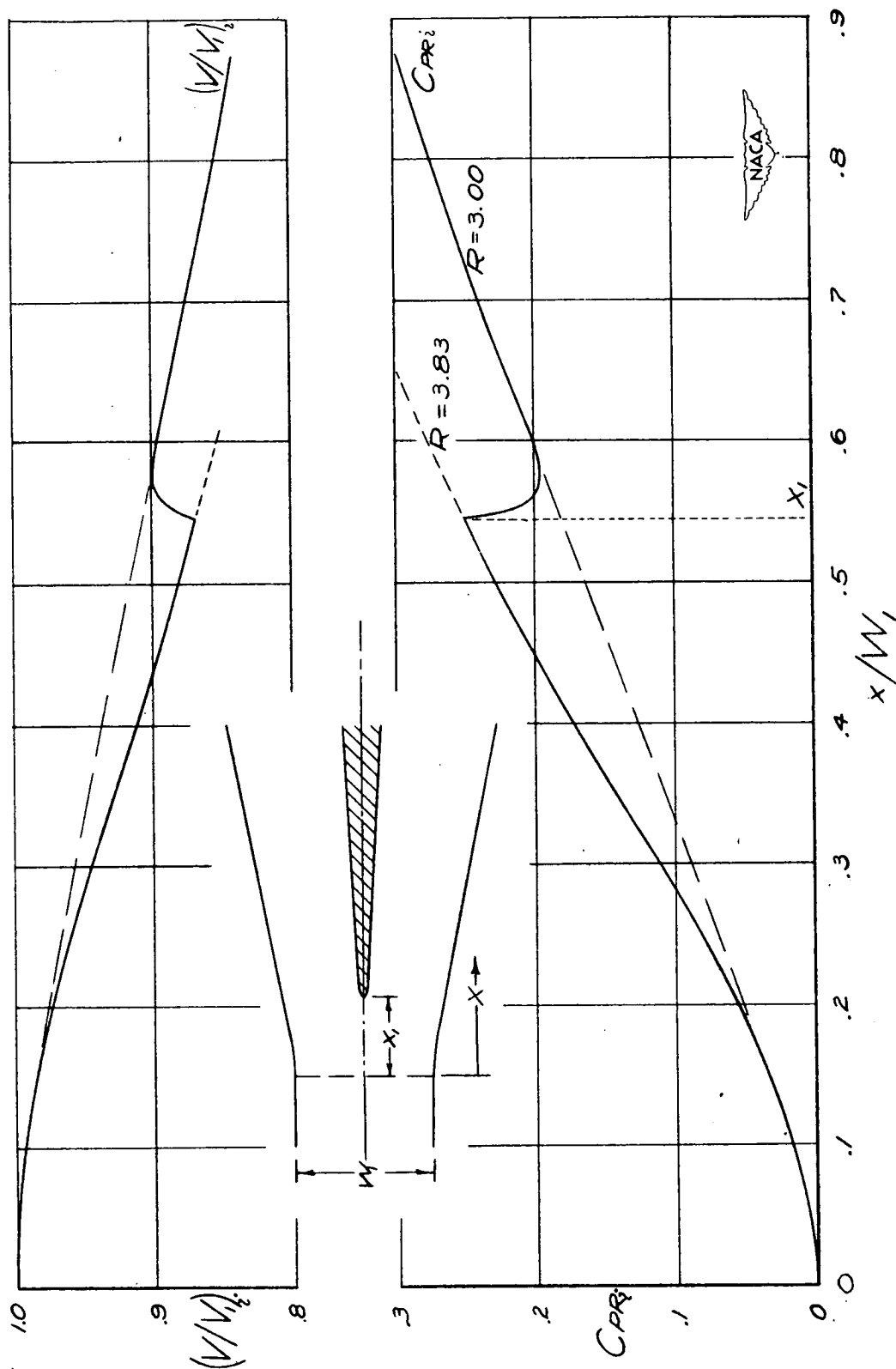


Figure 30.- Ideal variations of velocity and pressure ratios in diffuser with central wedge.  $L/W_1 = 7.75$ ;  $R = 3.0$ .